UPPSALA
UNIVERSITET

Digital Comprehensive Summaries of Uppsala Dissertations from the Faculty of Pharmacy 50

Pharmacokinetics and Pharmacodynamics of Oxycodone and Morphine with Emphasis on Blood-Brain Barrier Transport

EMMA BOSTRÖM

ACTA
UNIVERSITATIS
UPSALIENSIS
UPPSALA
2007

ISSN 1651-6192
ISBN 978-91-554-6840-8
urn:nbn:se:uu:diva-7772

Dissertation presented at Uppsala University to be publicly examined in B22, Biomedical Centre (BMC), Husargatan 3, Uppsala, Friday, April 20, 2007 at 13:15 for the degree of Doctor of Philosophy (Faculty of Pharmacy). The examination will be conducted in English.

Abstract
Boström, E. 2007. Pharmacokinetics and Pharmacodynamics of Oxycodone and Morphine with Emphasis on Blood-Brain Barrier Transport. Acta Universitatis Upsaliensis. *Digital Comprehensive Summaries of Uppsala Dissertations from the Faculty of Pharmacy* 50. 51 pp. Uppsala. ISBN 978-91-554-6840-8.

The pharmacokinetics and pharmacodynamics of oxycodone and morphine was investigated and related to the transport across the blood-brain barrier (BBB) in rats. The influence of a P-glycoprotein (P-gp) inhibitor on the plasma pharmacokinetics and pharmacodynamics of oxycodone was evaluated. Microdialysis experiments were conducted to evaluate the unbound pharmacokinetics, including the rate and extent of transport across the BBB, of oxycodone and morphine. Mathematical models were used to assess the pharmacokinetics and also the relationship between pharmacokinetics and pharmacodynamics of the drugs.

Oxycodone clearance, volume of distribution at steady-state, half-life, total brain tissue concentrations and tail-flick latency were all unaffected when a P-gp inhibitor was co-administered with oxycodone as compared to a control group. The lack of differences between the groups indicates that oxycodone BBB transport is not affected by P-gp inhibition. Investigating the unbound concentrations of oxycodone in brain and blood using microdialysis revealed an exciting finding. At steady-state, the unbound concentration in brain was 3 times higher than in blood (i.e. a $K_{p,uu}$ of 3), indicating that active influx is involved in the BBB transport of oxycodone. In contrast, the $K_{p,uu}$ of morphine was estimated to 0.56, which is an indication that active efflux mechanisms are involved in the BBB transport of morphine. This means that based on the same unbound concentration in blood, an approximately 6-fold higher unbound concentration of oxycodone compared to morphine will be reached in the brain. Using pharmacokinetic-pharmacodynamic modelling, the unbound brain concentrations of oxycodone and morphine were correlated to the tail-flick latency in vivo. The relative potency of the drugs was found to be concentration dependent with an infliction point of 55 nM.

In summary, this thesis emphasise the importance of taking the local brain pharmacokinetics into consideration when investigating the pharmacokinetics and the pharmacokinetic-pharmacodynamic relationships of centrally acting drugs.

Keywords: pharmacokinetics, pharamcodynamics, blood-brain barrier, oxycodone, microdialysis, NONMEM, brain distribution, transport

Emma Boström, Department of Pharmaceutical Biosciences, Division of Pharmacokinetics and Drug Therapy, Box 591, Uppsala University, SE-75124 Uppsala, Sweden

© Emma Boström 2007

ISSN 1651-6192
ISBN 978-91-554-6840-8
urn:nbn:se:uu:diva-7772 (http://urn.kb.se/resolve?urn=urn:nbn:se:uu:diva-7772)

To my family ♥

Papers discussed

This thesis is based on the following papers, which will be referred to by their Roman numerals in the text.

I **Boström E**, Jansson B, Hammarlund-Udenaes M and Simonsson USH. The use of liquid chromatography/mass spectrometry for quantitative analysis of oxycodone, oxymorphone and noroxycodone in Ringer solution, rat plasma and rat brain tissue.
Rapid Commun Mass Spectrom. 18:2565-76 (2004).

Copyright John Wiley & Sons Limited. Reproduced with permission.

II **Boström E**, Simonsson USH and Hammarlund-Udenaes M. Oxycodone pharmacokinetics and pharmacodynamics in the rat in the presence of the P-glycoprotein inhibitor PSC833.
J Pharm Sci. 94:1060-6 (2005).

Copyright John Wiley & Sons Incorporated. Reproduced with permission.

III **Boström E**, Simonsson USH and Hammarlund-Udenaes M. In vivo blood-brain barrier transport of oxycodone in the rat: indications for active influx and implications for pharmacokinetics/pharmacodynamics.
Drug Metab Dispos. 34:1624-31 (2006).

Reprinted with permission of the American Society for Pharmacology and Experimental Therapeutics. All rights reserved.

IV **Boström E**, Hammarlund-Udenaes M and Simonsson USH. Blood-brain barrier transport help explain discrepancies in *in vivo* potency between oxycodone and morphine
In manuscript

Contents

Abbreviations

ABC	ATP-binding cassette
A_{brain}	Amount of drug in brain tissue at steady-state
ATP	Adenosine triphosphate
$AUC_{0-\infty}$	Area under the concentration-time curve from time 0 until infinity
$AUC_{u,brain}$	Area under the unbound ISF concentration-time curve
$AUC_{u,blood}$	Area under the unbound blood concentration-time curve
AUEC	Area under the effect-time curve
$AUMC_{0-\infty}$	Area under the first moment-time curve from time 0 until infinity
BBB	Blood-brain barrier
BCSFB	Blood-cerebrospinal fluid barrier
BCRP	Breast cancer resistance protein
cAMP	Cyclic adenosine monophosphate
C_{blood}	Concentration in blood
C_{calc}	Calculated concentration at the last time point
C_{in}	Concentration of the microdialysis perfusate
CL	Clearance
CL_{in}	Influx clearance from blood to brain
CL_{out}	Efflux clearance from brain to blood
CNS	Central nervous system
C_{out}	Concentration of the microdialysis dialysate
C_{plasma}	Concentration in plasma
C_{RBC}	Concentration in red blood cells
CSF	Cerebrospinal fluid
$C_{tot,brain}$	Concentration in total brain tissue
C_{u}	Unbound concentration in blood
$C_{u,brain,ss}$	Unbound concentration in brain ISF at steady-state
$C_{u,blood,ss}$	Unbound concentration in blood at steady-state
CV	Coefficient of variation
$Dose_{iv}$	Intravenous dose
ECF	Extracellular fluid
FOCE INTER	First order conditional estimation with interaction method
f_{u}	Fraction unbound in plasma
GTP	Guanosine triphosphate
GTPγS	Guanosine-5′-O-(γ-thio)-triphosphate
H	Hematocrit
IS	Internal standard
ISF	Interstitial fluid
Iv	Intravenous

GLUT	Glucose transporter
k_0	Rate of the infusion
K_p	Equilibrium distribution ratio of drug between tissue and plasma based on total concentrations in tissue and plasma
$K_{p,u}$	Equilibrium distribution ratio of drug between tissue and blood based on total concentrations in tissue and unbound concentrations in blood
$K_{p,uu}$	Equilibrium distribution ratio of drug between tissue and blood based on unbound concentrations in tissue and blood
LC/MS/MS	Liquid chromatography tandem mass spectrometry
LLOQ	Lower limit of quantification
M3G	Morphine-3-glucorunide
M6G	Morphine-6-glucorunide
MRP	Multidrug resistant protein
OFV	Objective function value
PD	Pharmacodynamic
P-gp	P-glycoprotein
PK	Pharmacokinetic
PKPD	Pharmacokinetic / pharmacodynamic
PSA	Permeability surface area product
Q	Inter-compartmental clearance
QC	Quality control
RBC	Red blood cells
RSE	Relative standard error
SD	Standard deviation
SPE	Solid phase extraction
T	Time of the infusion
t½	Half-life
t_{last}	Last time point
TFA	Trifluoroacetic acid
V_{blood}	Volume of blood in brain
V_c	Central volume of distribution
V_{ss}	Volume of distribution at steady-state
$V_{u,brain}$	Unbound volume of distribution in brain
γ	Shape factor of the concentration-effect relationship
ε	Difference between observed and predicted observations
η	Difference between population and individual parameter estimate
θ	Typical value of a parameter
λ_z	Slope of the terminal phase of the concentration-time profile
σ^2	Variance of the εs
ω^2	Variance of the ηs

Introduction

The central nervous system (CNS) is the target of drug therapy for many therapeutic areas. The entry of a drug molecule from the blood to the brain is restricted by endothelial cells connected by tight junctions, the blood-brain barrier (BBB). In the case of a centrally acting drug, the passage across the BBB is essential for the pharmacological activity. However, for a peripherally acting drug, the entry across the BBB may cause CNS side effects and needs to be minimized. The function of the BBB is still not fully understood, and new insights into this area may give rise to new opportunities for drug development and delivery of centrally acting drugs to its site of action.

A variety of transport proteins are incorporated in the BBB. These include both efflux transporters, limiting the entry of molecules into the brain, and influx transporters that enhance the entry of molecules into the brain. Knowledge of the BBB transport properties is of importance when investigating the pharmacokinetics (PK) and pharmacodynamics (PD) of centrally acting drugs such as opioids.

Opioids are used to treat moderate to severe pain, which requires that a part of the systemically given dose must cross the BBB to reach the active sites within the CNS. Oxycodone and morphine are opioids that act at the μ-opioid receptors, and were used as the model substances in this thesis.

Opioids

Reference to opium was first made in the third century B.C., when Arabian traders introduced opium to the Orient, where it was used as an anti-diarrhoeal agent (Goodman and Gilman, 2001). Opium contains more than 20 alkaloids, including morphine and thebaine, the precursor of oxycodone. Today, the use of opioids is an essential part in the pharmacotherapy of moderate to severe pain (MacPherson, 2002).

Oxycodone (Fig. 1) has been used in the clinic since 1917, but has gained market shares especially in Finland and the United States during the past decades. Oxycodone is metabolized in the liver to several metabolites. The cytochrome P450 (CYP) enzyme CYP3A4 forms the main metabolite, noroxycodone (Fig. 1), and CYP2D6 forms an active metabolite, oxymorphone (Fig. 1). Oxymorphone has significantly higher μ-opioid receptor activation potency in *in vitro* agonist [^{35}S]-GTP-γS stimulated binding assays compared to oxycodone. Several other metabolites of oxycodone have also been reported. Among these, noroxymorphone is also more potent than oxycodone in *in vitro* agonist [^{35}S]-GTP-γS stimulated binding in hMOR1 cultured cells (Lalovic et al., 2006). There is limited information on to what extent the formation of active metabolites contributes to analgesia produced

by a dose of oxycodone. However, a recent investigation have shown that the contribution of oxymorphone and noroxymorphone antinociception to oxycodone analgesia is negligible (Lalovic et al., 2006).

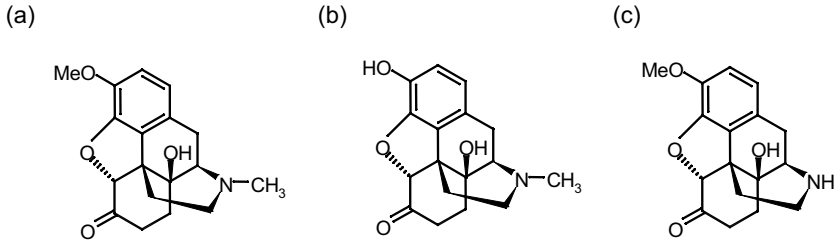

Figure 1. The molecular structures of oxycodone (a) and its metabolites oxymorphone (b) and noroxycodone (c).

Morphine (Fig. 2) has been extensively used over the past centuries as an antinociceptive agent, and is still considered the standard opioid agonist when it comes to moderate to severe pain (Goodman and Gilman, 2001). In man, morphine is metabolized to morphine-3-glucorunide (M3G) and morphine-6-glucorunide (M6G) (Fig. 2), while in rats only M3G is formed (Yeh et al., 1977; Oguri et al., 1990). M6G has shown to contribute to the analgesic effect of morphine in man (Murthy et al., 2002), while M3G does not seem to contribute to the analgesic effect of morphine in rats (Gardmark et al., 1998).

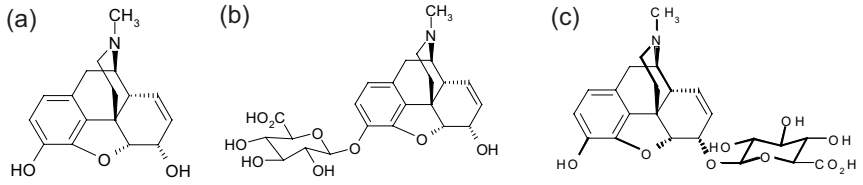

Figure 2. The molecular structures of morphine (a) and its metabolites morphine-3-glucorunide (b) and morphine-6-glucorunide (c).

The protein binding of oxycodone in human serum is 45 %, not too different from that of morphine (35 %) (Leow et al., 1993). Albumin is the major binding protein for both oxycodone and morphine (Leow et al., 1993). In rats, the protein binding of oxycodone and morphine is 26 and 60 %, respectively (Paper III and IV). The oral bioavailability in man is higher for oxycodone than for morphine, 60-87 % compared to 32 %, respectively (Leow et al., 1992; Poyhia et al., 1992; Westerling et al., 1995).

Oxycodone and morphine are used to treat similar pain conditions. There are however discrepancies in results of potency comparisons of the two drugs. When the two drugs were given intravenously (iv) in man, they were shown to be equipotent, that is, the same dose of morphine or oxycodone resulted in similar pain relief (Silvasti et al., 1998). After oral administration, a two-fold higher dose of controlled release morphine was needed compared to controlled release oxycodone to receive the same

effect (Curtis et al., 1999). In contrast, morphine was 10 times more potent than oxycodone when given epidurally after abdominal surgery (Backlund et al., 1997). In rats, after subcutaneous and intraperitoneal administration, oxycodone was two and four times more potent than morphine, respectively (Poyhia and Kalso, 1992). The opposite was observed when the drugs were administered intrathecally, with morphine being 14 times more potent than oxycodone (Poyhia and Kalso, 1992).

Opioid pharmacology

The opioids are ligands for the opioid receptors. The opioid receptors belong to the guanosine triphosphate (GTP) binding regulatory proteins, known as G-proteins (Goodman and Gilman, 2001). The opioid receptors are usually divided into three major subgroups, the μ, κ and δ – subtype, and are located at both central sites as the brain and spinal cord, as well as in the periphery (Goodman and Gilman, 2001; DeHaven-Hudkins and Dolle, 2004). The analgesic effects of opioids arise from their ability to inhibit the ascending transmission of nociceptive information from the dorsal horn of the spinal cord and to activate pain control circuits that descend from the midbrain to the spinal cord (Goodman and Gilman, 2001). Binding of the ligand inhibits adenylate cyclase and thereby reduce the intracellular cAMP content. Opioids also promotes opening of K^+ channels and suppresses opening of Ca^{2+} channels. These changes both inhibit the neuronal excitability and transmitter release, and thus the opioids are inhibitory at the cellular level.

Both oxycodone and morphine are selective for the μ-opioid receptor subtype (Lalovic et al., 2006; Peckham and Traynor, 2006). At the receptor level, morphine is more potent than oxycodone in *in vitro* [^{35}S]-GTP-γS binding assays, meaning that for a certain degree of receptor activation, a lower concentration of morphine compared to oxycodone would be needed (Thompson et al., 2004; Lalovic et al., 2006; Peckham and Traynor, 2006). In addition, morphine is slightly more efficacious than oxycodone *in vitro*, meaning that morphine can activate the receptor to a greater extent compared to oxycodone (Thompson et al., 2004; Lalovic et al., 2006; Peckham and Traynor, 2006).

The central nervous system

The central nervous system (CNS) consists of the brain and the spinal cord. The brain is responsible for processing most sensory information and coordinating body function. The spinal cord is the connection central for signals between the brain and the rest of the body.

The brain and spinal cord are cushioned in cerebrospinal fluid (CSF) that protects the CNS from outer damage. The CSF is secreted by choroid plexuses in the lateral, third and fourth ventricles (Davson and Segal, 1996). The neurons are surrounded by the interstitial fluid (ISF), also known as the extracellular fluid (ECF). The origin of the ISF is somewhat unclear, but it has recently been stated that the most likely source of mammalian brain ISF is from a combination of new filtration/secretion across the BBB together with some recycled CSF (Abbott, 2004). To maintain brain homeostasis and to regulate and limit the exchange of molecules between the blood

and the neuronal tissue or its fluid spaces, there are barriers present in the CNS. They include the BBB, formed by the endothelial cells of the capillary wall between the blood and the ISF, and the blood-CSF barrier (BCSFB) consisting of the choroid plexus epithelium localized between the blood and the ventricular CSF and the arachnoid epithelium between the blood and the subarachnoid CSF (Abbott, 2004). The surface area of the BBB is larger than that of the BCSFB, making BBB likely to be most important for drug delivery to the brain after systemic drug administration.

The blood-brain barrier

The function of the BBB is to maintain the microenvironment of the brain and to protect it from toxic molecules. On its passage from the blood to the brain, a drug molecule has to pass two membranes of the endothelial cell; the luminal membrane facing the blood and the abluminal membrane facing the brain (Fig. 3). The BBB is characterized by the tight junctions between the endothelial cells, making paracellular (between cells) passage of drugs very restricted. Lack of fenestrations and few pinocytotic vesicles further limit the transport across the BBB (Tamai and Tsuji, 2000). This means that only very small hydrophilic molecules can pass via the paracellular pathway (van Bree et al., 1988). All other molecules must pass the endothelial cell by the transcellular (across the cell) path, in order to reach the brain and exert their pharmacological effects. A summary of different ways to cross the BBB is presented in Fig. 3, and is described in more detail below.

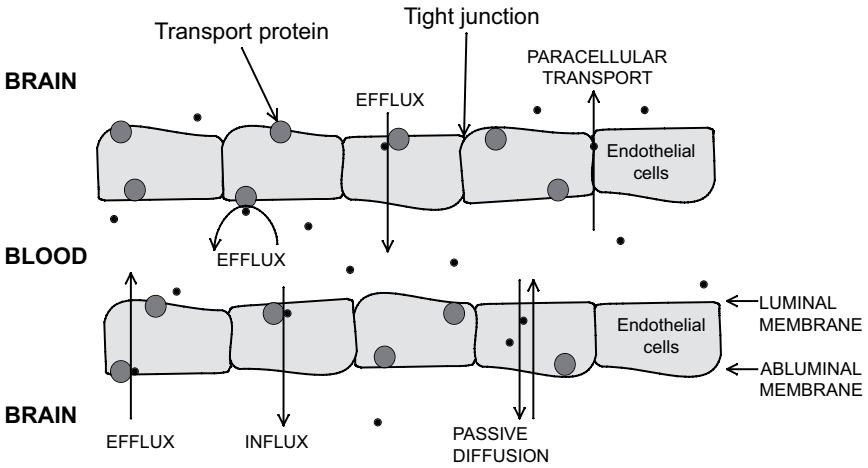

Figure 3. Mechanisms of blood-brain barrier transport include passive diffusion and carrier mediated transport. Passive diffusion occurs when the molecules are passing across the cell membrane without interaction with a transporter. Passive diffusion is a random movement of molecules with a net direction towards a lower concentration. In carrier mediated transport, a transporter is involved in the passage across the membrane. The carrier mediated transport can be divided into energy-independent facilitated diffusion and energy-dependent active transport. Carrier mediated transport can have the direction from blood to brain (influx transport) or from brain to blood (efflux transport).

BBB transport processes

Passive diffusion

The transport of a molecule across a cell membrane by passive diffusion is energy independent and can not be saturated. There are three major determinants that influence the passive diffusion of a molecule, namely size, charge and lipophilicity. A large, hydrophilic and charged molecule will diffuse at a lower rate than a small, hydrophobic and uncharged compound. Diffusion is a random movement of molecules, but has a net direction of movement towards lower concentrations, in order to reach equilibrium.

Carrier mediated transport

Carrier mediated transport can be saturated and is substrate specific, which discriminates it from passive diffusion. When a substrate bind to a carrier, the resulting substrate/carrier complex undergoes a conformational change. This allows the substrate to traverse the membrane and to be released on the opposite side of the membrane. Depending on the direction of transport across the BBB, the transporters are either called influx or efflux transporters. Influx transporters enhance the transport of drugs from blood into the brain, while efflux transporters enhance the transport of drug from brain to blood or hinders drug to enter the brain tissue. The transport of a molecule across a membrane by carrier mediated transport can be independent of energy (facilitated diffusion) or energy dependent (active transport).

Facilitated diffusion

An example of facilitated diffusion is the uptake of glucose by the GLUT-1 transporter in blood-tissue barriers including BBB (Pessin and Bell, 1992). By facilitated diffusion, a molecule is exchanged from high concentration in the blood to low concentration in the tissue, which resembles passive diffusion. GLUT-1 have been proposed to be involved in the BBB transport of M6G (Bourasset et al., 2003).

Active transport across the BBB

Energy is needed to move a molecule across a membrane from low concentration to high concentration. For example, the intracellular composition of solutes differs from their concentration in the ISF. To maintain this "unequilibrium", the presence of active transporters is necessary.

Active transport can be carried out by the use of adenosine triphosphate (ATP). Among others, these transporters include the Na/K-ATPase that maintain and generate the steady-state gradients of Na^+ and K^+ in the cells, and transporters belonging to the ATP-binding cassette family, the ABC transporters. The most well known ABC transporter is the efflux transporter P-glycoprotein (P-gp) that is located in the luminal membrane of the BBB and limits the entry of many drugs into the brain. Several opioids have been reported to be substrates of P-gp, including morphine, methadone and loperamide (Letrent et al., 1998; Skarke et al., 2003;

Wang et al., 2004).

The presence of transporters in the BBB has implications for the PK and PD of a drug (Hammarlund-Udenaes et al., 1997). For example, if a drug that is a P-gp substrate is co-administered with P-gp inhibitor, the brain concentrations of the drug will increase. If the drug has a target CNS effect, a higher effect than what could be anticipated without the P-gp inhibitor is achieved. However, blocking of P-gp may lead to unwanted central side-effects for drugs such as the second generation antihistamines (Polli et al., 2003).

PK considerations of BBB transport

Collection of plasma samples is the most common and practical way to measure drug concentrations in the body. However, when investigating the BBB transport of drugs, information on unbound drug concentrations from both sides of the BBB is favorable, which the regular plasma samples do not provide. It is therefore of interest to measure the unbound drug concentrations in blood as well as in the brain ISF.

Studying the PK aspects of BBB transport, three aspects should be considered; rate of transport, extent of transport and binding of drug within the brain.

Rate of transport

The rate of transport across the BBB is a measure of the permeability clearance across the BBB (µL/min·g brain). The parameters used to describe the rate of transport include the permeability surface area product (PSA) and the influx clearance (CL_{in} or K_{in}). The influx clearance describes the net capacity of the BBB to transport a molecule into the brain, i.e. the combined impact of passive diffusion and possible influx and efflux transport mechanisms. The rate of transport across the BBB from brain to blood can be described by the efflux clearance CL_{out}, which describes the combined impact of passive diffusion and possible efflux and influx transport systems.

Extent of transport

The extent of BBB transport can be described with the relationship of unbound drug concentrations in brain to that in blood, $K_{p,uu}$, which can be calculated according to the following equations:

$$K_{p,uu} \rceil \frac{C_{u,brain,ss}}{C_{u,blood,ss}} \quad (1)$$

$$K_{p,uu} \rceil \frac{AUC_{u,brain}}{AUC_{u,blood}} \quad (2)$$

$$K_{p,uu} \approx \frac{CL_{in}}{CL_{out}} \quad (3)$$

$C_{u,brain,ss}$ and $C_{u,blood,ss}$ are the unbound steady-state concentrations of drug in brain and blood, respectively. $AUC_{u,brain}$ and $AUC_{u,blood}$ are the areas under the unbound concentration vs. time curves for brain and blood, respectively, while CL_{in} and CL_{out} are the unbound influx and efflux clearances across the BBB, respectively.

$K_{p,uu}$ can also be thought of as the net flux. The net flux is the sum of all transport processes at the BBB, including passive diffusion as well as carrier mediated transport by efflux and influx transporters. If the unbound concentration in the brain at steady-state is below that of the blood, $K_{p,uu}$ will be below one. This means that the net flux across the BBB is dominated by active efflux transport or substantial influence of bulk flow or brain metabolism, clearing the substance from the brain tissue. A $K_{p,uu}$ above one means that the net flux is dominated by active influx transport across the BBB, while a $K_{p,uu}$ of unity means that the BBB transport takes place by passive diffusion, or that the influx and efflux mechanisms have the same impact on the BBB transport.

Binding within the brain

The binding within the brain can be described by the unbound volume of distribution in the brain, denoted $V_{u,brain}$, and is calculated as follows:

$$V_{u,brain} \approx \frac{A_{brain} \cdot V_{blood} \cdot C_{blood}}{C_{u,brain,ss}} \quad (4)$$

where A_{brain} is the total amount of drug per gram of brain at steady-state. V_{blood} is the volume of blood per gram of brain. $C_{u,brain,ss}$ is the unbound brain ISF concentration at steady-state. C_{blood} is the total concentration in blood which can be derived by multiplying the plasma concentration with the partitioning between blood and plasma (C_{blood}/C_{plasma}).

Methods to study BBB transport

A range of *in vitro* and *in vivo* methods can be used to study the transport of drugs across the BBB including influence of transporters.

Cultured brain endothelial cell lines can be used to identify the specific transporters that act on a drug. However, many drugs are transported by more than one transporter which makes it difficult to draw conclusions on the contribution of each transporter *in vivo*. Also, an *in vitro* setting can never totally resemble the *in vivo* situation with all endogenous substances present, making *in vivo* experiments necessary at least for confirmation of *in vitro* results.

In situ methods used to assess the rate of BBB transport include the brain uptake index method (Oldendorf, 1970), the brain efflux index method (Kakee et al., 1996),

the *in situ* brain perfusion technique (Takasato Y. Rapoprt), and the *in vivo* methods iv injection technique (Ohno et al., 1979) and microdialysis (Ungerstedt, 1991; Elmquist and Sawchuk, 1997). To assess the extent of BBB transport, microdialysis could be used.

Animal models can be used to study the *in vivo* situation of BBB transport. Knock-out animals that lack the gene that codes for a certain transporter can be used. For example, the impact of P-gp on BBB transport of various drugs have been studied using the multi drug resistance knockout mice (Thompson et al., 2000; Dagenais et al., 2001). This provides information on the specific transporter that is involved in the transport of a drug *in vivo*. However, there are still uncertainties whether the knock-out animals are exactly like the wild-type, except for the lack of transporter. It has been reported that the mRNA expression of the gene coding for breast cancer resistance protein (BCRP) is increased in mice lacking P-gp (Cisternino et al., 2004).

Another possibility to study the BBB transport properties of a drug is to co-administer a transporter inhibitor together with the drug. The main disadvantage with the use of an inhibitor is a possible lack of specificity for the transporter studied. For example, the cyclosporine analogue PSC833 (Valspodar) was for a long time considered to be an inhibitor of P-gp only. However, also BCRP and multidrug resistant protein 2 (MRP2) are inhibited by PSC833 (Chen et al., 1999; Eisenblätter et al., 2003).

Microdialysis

Over the past couple of decades, microdialysis has been developed and recognized as a valuable tool in investigations of drug distribution to the CNS (de Lange et al., 1995; Hammarlund-Udenaes, 2000; Sawchuk and Elmquist, 2000; Deguchi, 2002). The main advantage of microdialysis is that it provides a possibility for obtaining unbound drug concentrations in several tissues or fluids in one individual over time. Thus, when investigating the time course of BBB transport and PKPD of drugs that act at receptors facing brain ISF, microdialysis is a valuable tool.

The microdialysis probe is composed of a semi-permeable membrane that allows passage of solutes and molecules that are smaller than the cut-off value of the membrane. After implantation into the tissue or fluid of interest, the probe is perfused by a solution that closely resembles the ISF, the perfusate. The fluid leaving the probe, the dialysate, is collected in fractions. Due to the continuous flow of the perfusate, a concentration gradient along the microdialysis probe is created. Depending on the direction of the concentration gradient, molecules will either be delivered to, or recovered from, the ISF surrounding the probe. The fraction of the concentration that is recovered from the tissue is referred to as the relative recovery. Preferably, the recovery of each individual probe should be estimated *in vivo*. By using the *in vivo* recovery, a quantitative measure of the true unbound concentration in a tissue can be obtained.

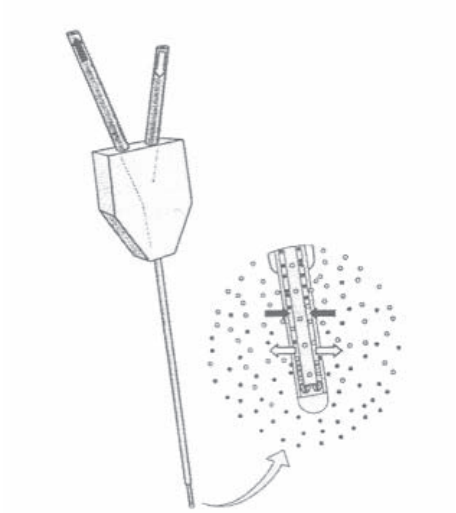

Figure 4. The principle of microdialysis. The perfusate enters through the inner cannula to the tip of the probe, where a semi permeable membrane allows exchange between the perfusate and the surrounding tissue before collected in fractions (Ungerstedt, 1991).

The methods described for estimation of the *in vivo* recovery include the no-net flux (Lonnroth et al., 1987), retrodialysis by drug (Bouw and Hammarlund-Udenaes, 1998) and retrodialysis by calibrator (Wang et al., 1993). When using retrodialysis by drug or by calibrator, it is assumed that the fraction of drug that leaves the probe perfusate is the same as the fraction that enters into the probe perfusate. This may not always be the case and needs to be checked *in vitro* before performing *in vivo* experiments. Using retrodialysis by drug, the drug of interest is perfused through the probe for some time, followed by a wash-out period and thereafter drug is administered to the animal. This means that the recovery is assumed to be constant during the study period. Using retrodialysis by calibrator, the calibrator is present in the perfusate during all of the experiment, and possible changes in the recovery during the experiment can be evaluated. The calibrator should resemble the drug of interest as much as possible, which make a deuterated analogue an attractive choice. The use of a deuterated analogue, however, requires the possibility to analyze the dialysate fractions with mass spectrometry.

There are some drawbacks with the microdialysis method. Not all substances are possible to study with microdialysis. Especially lipophilic molecules may stick to the probe membrane or tubings in the experimental setup. A high protein binding of the drug will put high demand on the sensitivity on the analytical assay. The technique is technically demanding, with rather complicated surgery including probe implantation. Also, the tissue trauma and possible loss of BBB integrity after probe implantation is often discussed. One investigation have shown that the BBB permeability was affected 24 h after probe implantation (Groothuis et al., 1998). In contrast, another investigation conclude that local cerebral blood flow and glucose metabolism were nearly normalized 24 h after probe implantation (Benveniste et al., 1987).

Modelling

Mathematical models can be used to describe how drug concentrations changes over time, or how drug response relates to drug concentrations or exposure. In the population modelling approach, all data is analysed simultaneously and therefore information from all individuals is shared.

Population modelling utilizes non-linear mixed effects models. The term "mixed" refer to that both fixed and random effects are included into the model. An individual parameter (CL_i) can be described by:

$$CL_i = \theta_{CL} \cdot e^{\eta_i} \quad (5)$$

The subscript i represent the i^{th} individual, the fixed effect parameter θ_{CL} denotes the typical value of CL in the population, and η_i is a random effect that describes the inter-individual variability (IIV) i.e. the individual difference from the typical value. The η_i values are assumed to be normally distributed, with a mean of 0 and a variance of ω^2.

The residual error (ε) is a random effect that describes the difference between the observed and predicted observation. The residual error may be the result of chemical assay errors, errors in dose or sampling time, or model misspecification. In Eq. 6, an additive model is used to account for the residual error:

$$C_{obs,ij} = C_{pred,ij} + \varepsilon_{ij} \quad (6)$$

$C_{obs,ij}$ is the j^{th} observation of the i^{th} individual, $C_{pred,ij}$ is the corresponding predicted concentration and ε_{ij} is the residual error for that observation. The residual error is assumed to be normally distributed around zero with a variance of σ^2.

Aims of the thesis

The general aim of this thesis was to investigate the role of the BBB transport in the PK and PD of oxycodone in rats.

The specific aims were:

- to develop and validate a sensitive and specific analytical method for the quantification of oxycodone and its metabolites oxymorphone and noroxycodone in microdialysates from brain and blood, rat plasma and rat brain tissue using LC/MS/MS

- to investigate whether oxycodone is a P-gp substrate or not by studying the impact of a P-gp inhibitor (PSC833) on the plasma PK of oxycodone, total brain tissue oxycodone concentrations and antinociception measured by the tail-flick method in the rat

- to investigate the BBB transport and unbound PK of oxycodone using microdialysis, including quantification of the rate and extent of BBB transport

- to investigate the importance of BBB transport for the PKPD relationships of oxycodone and morphine by the use of nonlinear effects modelling

Materials and Methods

Animals

Male Sprague-Dawley rats (B&K, Sollentuna, Sweden) were used in the animal experiments. The animals were group housed at 22º C with a 12 hour light / dark cycle for at least five days prior to surgery. Standard diet and water were available *ad libitum*. At the day of surgery, the animals were weighing 250-320 g. The studies were approved by the Animal Ethics Committee of Tierp District Court, Tierp, Sweden (C 246/1, C 247/1, C 176/4 and C 177/4).

Animal surgery

The rats in Paper II, III and IV were anaesthetized by inhalation of enfluran (Efrane®, Abbott Scandinavia AB, Kista, Sweden) or isofluran (Isofluran Baxter®, Baxter Medical AB, Kista, Sweden). During the surgical procedure, the rat body temperature was maintained at 38°C by using a CMA/150 temperature controller (CMA, Stockholm, Sweden). A PE-50 cannula fused with silastic tubing was inserted into the left femoral vein for drug administration. A PE-50 cannula fused with PE-10 tubing was inserted into the femoral artery for blood sampling. In order to avoid clotting the catheters were filled with a heparinised saline solution (Heparin Leo®, 100 IE/mL, Leo Pharma AB, Malmö, Sweden).

In addition, for the microdialysis animals in Paper III and IV, a CMA/20 blood probe (10 mm, CMA, Stockholm, Sweden) was inserted into the right jugular vein through a guide cannula and fixed to the pectoralis muscle with two sutures. The anaesthetized rat was placed into a stereotaxic instrument (David Kopf Instruments, Tujunga, USA) for the implantation of the brain probe. A midsaggital incision was made to expose the skull, and the CMA/12 guide cannula was implanted into the striatum with the coordinates 2.7 mm lateral and 0.8 mm anterior to the bregma and 3.8 mm ventral to the surface of the brain. After insertion the guide cannula was anchored to the scull with a screw and dental cement (Dentalon® Plus, Heraeus, Hanau, Germany). A CMA/12 probe (3 mm, CMA, Stockholm, Sweden) was inserted into the striatal guide. A piece of PE-50 tubing was looped subcutaneously on the back of the rat to the surface of the neck in order to let the perfusion solution adjust to body temperature before entering the brain probe.

For all animals, the ends of the cannulae and catheters were passed subcutaneously to a plastic cup placed on the posterior surface of the neck out of reach from the rat. The rats were placed in a CMA/120 system for freely moving animals (CMA, Stockholm, Sweden) with free access to water and food, and were allowed to recover

for approximately 24 hours before the experiment. All experiments were performed at the same time of the day.

Experimental procedures

Study designs

A summary of the drugs and doses studied are presented in Table 1. In Paper II, half of the animals (n = 8) were given the P-gp inhibitor PSC833 dissolved in triethylene glycol and ethanol, 40:10 (v/v). PSC833 was administered as a bolus dose, immediately followed by a constant rate infusion for the entire experiment. The other half of the animals (n = 8) received the vehicle without PSC833 in the same manner. One hour after the start of PSC833 or vehicle administration, a 60 min constant rate iv infusion of oxycodone was started. Eight blood samples were withdrawn pre-dose, during the infusion and up to 180 minutes after the start of the infusion from each animal. Tail-flick latency was recorded and at the end of the experiment, the animals were decapitated. Methadone has been shown to be a P-gp substrate and was used as a positive control in Paper II (Wang et al., 2004). Methadone was administered to two animals, one receiving PSC833 and the other the vehicle in the same manner as the animals receiving oxycodone.

Table 1. *Summary of the drugs and doses investigated.*

Paper	Drug	Dose	Time of infusion
II	oxycodone	0.3 mg/kg/h	60 min
	oxycodone + PSC833	0.3 mg/kg/h + 2.3 mg/kg bolus and 1.06 mg/kg/h	60 min + 240 min
III	oxycodone[a]	0.227 mg/kg bolus + 0.533mg/kg/h	120 min
	oxycodone[a]	0.3 mg/kg/h	60 min
IV	morphine[a]	0.9 mg/kg/h	60 min
	oxycodone[b]	0.3 mg/kg/h	60 min
	morphine[b]	0.9 mg/kg/h	60 min

[a] Microdialysis experiment, [b] Total brain tissue experiment

The experimental setup for the microdialysis experiments in Papers III and IV is presented in Fig. 5. Both microdialysis probes (blood and brain) were perfused with Ringer solution (147 mM NaCl, 2.7 mM KCl, 1.2 mM $CaCl_2$ and 0.85 mM $MgCl_2$). In Paper III, D3-oxycodone (45 ng/mL) was used as a calibrator and were dissolved in the Ringer solution and perfused through the probes for recovery estimation. In Paper IV, D3-morphine (105 ng/mL) was used as a calibrator, and in the control group, blank Ringer solution without calibrator was used to perfuse the microdialysis probes. The probes were perfused at a flow rate of 1 µl/min. Samples were collected in 15 min intervals during a 60 min stabilization period.

In Paper III, two infusion regimens of oxycodone were applied. The first group of animals (n = 10) received 0.3 mg/kg (0.951 µmol/kg) oxycodone given as a 60

min constant rate infusion in the left femoral vein. Brain and blood dialysates were collected as 10 min fractions during the infusion and for the first hour after the stop of the infusion. Thereafter the dialysates were collected in 20 min intervals for the last two hours of the experiment. The second group (n = 10) received an oxycodone infusion as a bolus dose of 0.277 mg/kg (0.878 µmol/kg) over 10 s followed by a 120 min constant rate infusion of 0.533 mg/kg/h (1.69 µmol/kg/h) in the left femoral vein. Brain and blood dialysates were collected as 10 min fractions during the first hour of the infusion and as 20 min fractions for the second hour of the infusion. Five rats were given an overdose pentobarbital just before the end of the infusion and were decapitated for quantification of total brain tissue oxycodone concentrations at steady-state for determination of $V_{u,brain}$. For the remaining five animals, dialysates were collected as 10 min fractions for the first hour after the stop of the infusion and as 20 min fractions for the second hour after stop of the infusion.

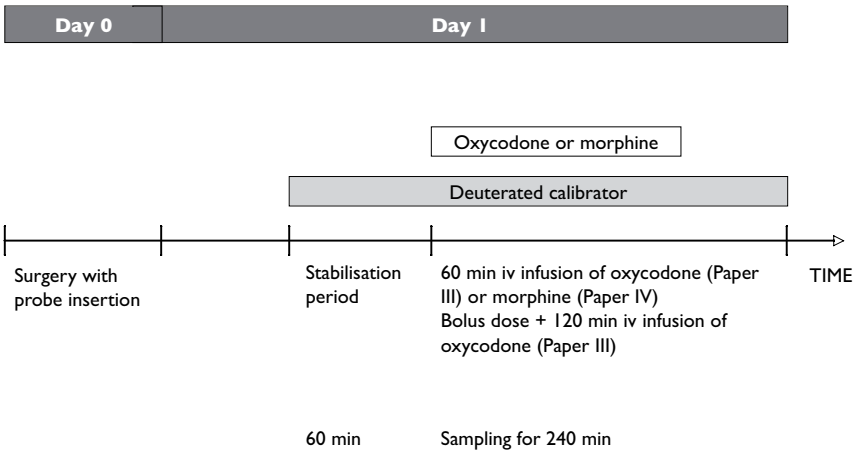

Figure 5. A schematic picture of the experimental setup for the microdialysis experiments to investigate the blood-brain barrier transport of oxycodone and morphine in Paper III and IV.

In Paper IV, morphine was administered as a 60 min constant rate infusion of 0.9 mg/kg (3.154 µmol/kg) (n = 9). Brain and blood dialysates were collected as 10 min fractions during the infusion and for the first hour after the stop of the infusion. Thereafter the dialysates were collected in 20 min intervals for the last two hours of the experiment.

One to eight blood samples from each microdialysis rat in Papers III and IV were collected into heparinised vials. No more than 2 mL of blood was collected from each rat.

The time-course of total brain tissue concentrations of oxycodone and morphine was evaluated. The rats were divided into two groups. The rats received either 0.3 mg/kg (0.951 µmol/kg) oxycodone or 0.9 mg/kg (3.154 µmol/kg) morphine given as a 60 min constant rate infusion in the left femoral vein. At 10, 30, 60, 90, 120, 180 and 240 min (n = 3 per time point), the rats were sacrificed with an overdose of pentobarbital and decapitated. All brain samples were frozen at -20°C until analysis.

Sample treatment

After the end of each collection interval, microdialysate vials were capped and stored at -20°C. The blood samples were collected into heparinised vials and centrifuged at 10 000 rpm for 7 minutes. The plasma was transferred to clean vials and kept at -20°C until analysis. The brain tissues of the microdialysis animals in Paper III and IV were examined for any extensive bleeding. All brain tissues from Papers II-IV were frozen at -20°C until chemical assay.

Antinociceptive measurements

In Paper II and IV, the antinociceptive effect of oxycodone and morphine was evaluated using the hot water tail-flick method. A mark was made 6 cm from the distal tip of each rat's tail to ensure comparable exposure to heat. The tail was put into a water bath maintained at 50°C. The time from placing the tail into the water, until it was voluntarily moved was recorded as the tail-flick latency. A cut-off time of 15 s was applied to avoid tissue damage.

Microdialysis probe recovery

Blood and brain microdialysis probes were calibrated using a deuterated analogue of oxycodone (Paper III) and morphine (Paper IV). The calibrators were present in the perfusion fluid during all of the experiment, making possible variations in the recovery during the experiment detectable. The recoveries of the drugs were calculated according to Eq. 7.

$$Recovery_{in\ vivo} = \frac{\sum_{i=1}^{x} \left(1 - \frac{C_{out,i}}{C_{in}}\right)}{x} \qquad (7)$$

C_{in} is the concentration of the calibrator in the perfusate entering the probe, and $C_{out,i}$ is the concentration of the calibrator in the i^{th} dialysate fraction exiting the probe. The average recovery for each probe was estimated based on the recovery in each dialysate fraction.

Blood to plasma partitioning

The partitioning between blood and plasma for oxycodone in rats was investigated *in vitro*. Fresh blood from rats was collected in heparinised vials and spiked with two concentrations of oxycodone (50 ng/mL and 500 ng/mL). The experiments were performed in duplicate. The vials were placed in a water bath maintained at 37°C and were gently tilted. Samples were taken from the vials between 0 and 60 min, followed by immediate centrifugation. After centrifugation the plasma layer was separated from the red blood cell (RBC) layer and both layers was immediately frozen at -20°C until analysis.

Chemical assay

Oxycodone and metabolites

In Paper I, selective and sensitive liquid chromatographic methods using tandem mass spectrometry detection (LC/MS/MS) were developed. The methods were able to quantify oxycodone, D3-oxycodone, noroxycodone and oxymorphone in Ringer (Method I), rat plasma (Methods II and III) and rat brain tissue (Method IV), respectively. The methods were used to analyze samples containing oxycodone and D3-oxycodone (Papers II-IV).

The LC/MS/MS system consisted of an LC-10AD pump (Shimadzu, Kyoto, Japan) and a Triathlon 900 auto sampler (Spark Holland, The Netherlands) equipped with a 100 µL loop and a Zorbax SB-CN column (4.6 x 150 mm, Agilent Technologies, Wilmington, DE, USA). The column was maintained at 50°C and a constant flow rate of 1.0 ml/min was employed. The flow was splitted allowing 0.2 ml/min to enter the MS (Quattro Ultima, Micromass Manchester, United Kingdom). The mobile phase consisted of 45% acetonitrile in 5 mM ammonium acetate. The MS was used in the positive electrospray mode. The transition modes for the drugs are summarized in Table 2. MS control and spectral processing were carried out using MassLynx software, version 4.0 (Micromass, Manchester, United Kingdom). The MS settings that gave the best resolution and highest sensitivity were selected and are presented in Table 3.

Table 2. *The transition modes of the analytes in Paper I.*

Substance	Transition mode	Internal Standard
oxycodone	m/z 316.1 → m/z 297.9	D6-oxycodone
D3-oxycodone	m/z 319.1 → m/z 301	D6-oxycodone
oxymorphone	m/z 302.2 → m/z 284	D3-oxymorphone
noroxycodone	m/z 302.2 → m/z 284	D3-noroxycodone
D6-oxycodone	m/z 322.15 → m/z 304	
D3-oxymorphone	m/z 305.2 → m/z 287	
D3-noroxycodone	m/z 305.2 → m/z 287	

Table 3. *The mass spectrometer settings that were used in the analytical method presented in Paper I.*

Parameters	
Desolvation temperature (°C)	400
Source temperature (°C)	120
Cone gas flow (L/h)	200
Desolvation gas flow (L/h)	800
Collision gas pressure (Torr)	$3 \cdot 10^{-3}$
Capillary voltage (kV)	1.2
Cone voltage (V)	30

Standard and quality control sample preparations

In Method I, oxycodone, D3-oxycodone, noroxycodone and oxymorphone were dissolved in blank Ringer solution and a standard curve in the range of 0.5-150 ng/mL for all compounds was prepared. Quality control (QC) samples of 1.88, 62.8 and 125.5 ng/mL were prepared.

For Methods II and III, blank rat plasma was spiked with oxycodone, noroxycodone and oxymorphone. The standard curve was prepared in the range of 0.5-250 ng/mL, and the concentrations of the QC samples were 1.45, 48.5 and 194 ng/mL.

For Method IV, the blank brain tissue sample was prepared by homogenization of drug-free brain tissue with a 5-fold volume (w/v) of 0.1 M perchloric acid. After centrifugation, the supernatant was used for further extraction. The calibration standards were prepared by spiking of oxycodone, noroxycodone and oxymorphone to drug-free brain tissues. The tissues were homogenized with a 5-fold volume of 0.1 M perchloric acid (w/v) subtracted by the volume of the added analytes. After centrifugation, the supernatant was used for further extraction. The standard curve range in the rat brain tissue was from 4-1000 ng/g brain for noroxycodone and oxymorphone and from 20-1000 ng/g brain for oxycodone. QCs were prepared at 25, 125 and 750 ng/g brain.

Standard and QC samples were stored at -20°C until analysis. Working solutions of the internal standards (ISs) (D6-oxycodone, D3-noroxycodone and D3-oxymorphone) were prepared in water for Methods I, III and IV, and in acetonitrile for Method II.

Sample preparation

In Method I, Ringer samples were analyzed for oxycodone, D3-oxycodone, noroxycodone and oxymorphone. The samples were diluted with an equal volume of water spiked with the ISs at concentrations of 40 ng/mL, vortexed for 5 s where after 16 µl was injected onto the column.

In Method II, rat plasma samples were analyzed for oxycodone and oxymorphone. Fifty µl of plasma was precipitated with 100 µl acetonitrile spiked with the ISs at a concentration of 30 ng/mL and vortexed for 5 s. After centrifugation at 10 000 rpm for 5 min, 30 µl of the supernatant was injected onto the column.

In Method III, rat plasma samples were analyzed for oxycodone, noroxycodone and oxymorphone. One hundred µl rat plasma were purified using a slightly modified previously reported solid phase extraction (SPE) method (Joel et al., 1988). After evaporation of the eluate, the residue was dissolved in the mobile phase and 30 µl were injected onto the LC/MS/MS system.

In Method IV, the brain tissues were homogenized with a 5-fold volume of 0.1 M perchloric acid. After centrifugation, 100 µl of the supernatant was purified using the same SPE method as in Method III.

In Paper III, the red blood cells (RBCs) were prepared according to a previously described method (Dumez et al., 2005). The RBCs were diluted with four times its volume with distilled water. After 5 min, the solution was vortexed and thereafter centrifuged at 10 000 g to precipitate the cell debris. Four hundred µl of the solution was conducted to the same SPE procedure as for the brain homogenate in Method IV.

Validation

For each method in Paper I, the accuracy and intra-day precision was determined in one validation run. This run included a standard curve, QC samples (n=6) from each concentration and six replicates of the lower limit of quantification (LLOQ) samples. The inter-day precision was determined by analyzing six QC samples of each concentration interspersed with unknown study samples at three separate occasions. The precision was determined by calculation the standard deviation as a percentage of the average (coefficient of variation, CV). The accuracy was determined as the percentage of the added concentration. The LLOQ was determined as the lowest concentration that could be analysed with a CV<20 % and an accuracy of 80-120 %.

Morphine

In Paper IV, the samples containing morphine and D3-morphine were analyzed according to a previously described method, with some modifications (Bengtsson et al., 2005). D3-morphine was used as the microdialysis calibrator in the microdialysis experiments or as the IS in the analysis of the plasma and brain tissue samples. The LC/MS/MS system consisted of two LC-10AD pumps (Shimadzu, Kyoto, Japan) and a Triathlon 900 auto sampler (Spark Holland, The Netherlands) equipped with a 100 µL loop. A HyPurity C18 guard column, 10 x 3 mm, 3 µm particle size (Thermo Hypersil-Keystone, PA, USA) was used for purification. In the plasma and brain tissue methods, an in-line filter, A-431, 0.5 µm (Upchurch Scientific, WA, USA), was placed before the guard column. A ZIC HILIC column, 50 x 4.6 mm, 5 µm particle size (SeQuant AB, Umeå, Sweden) was utilized for the analytical separation. Both pumps were set to a flow of 0.5 mL/min. One pump was used for purification with 0.02 % trifluoroacetic acid (TFA) and the other was used for analytical separation with 70 % ACN in 5 mM ammonium acetate. The transition modes were m/z 286 → 152 for morphine and m/z 289 → 152 for D3-morphine. MS control and spectral processing were carried out using MassLynx software, version 4.0 (Micromass, Manchester, United Kingdom).

No sample pretreatment was needed for the microdialysis samples, and a volume of 5 µL was directly injected onto the column-switching system. Fifty µL of plasma was precipitated with 100 µL acetonitrile containing IS (D3-morphine, 25 ng/mL), vortexed and centrifuged. Thereafter 50 µL of the supernatant was evaporated under a stream of nitrogen at 45°C, and the residue was dissolved in 200 µL 0.02 % TFA by vortex mixing and ultra-sonication. The injection volume was 10 µL. The brain tissue samples were homogenized centrifuged and subject to SPE in the same manner as the oxycodone brain tissue samples. The residue was dissolved in 200 µL of the mobile phase and 10 µL was injected onto the column.

Data analysis

Non compartmental analysis

In Paper II, the individual clearance (CL) and volume of distribution at steady state (V_{ss}) were calculated according to Eq. 8 and 9, respectively.

$$CL = \frac{Dose_{iv}}{AUC_{01\Omega}} \quad (8)$$

$$V_{ss} = \frac{k_0 \cdot T \cdot AUMC_{01\Omega}}{AUC_{01\Omega}^{2}} - \frac{T(k_0 \cdot T)}{2 \cdot AUC_{01\Omega}} \quad (9)$$

$AUC_{0-\infty}$ is the area under the plasma concentration versus time curve from time zero until infinity which is the sum of the area under the concentration versus time curve until the last observation (AUC_{0-t}) and the residual area ($AUC_{t-\infty}$) The residual area was determined as the calculated concentration at the last time point (C_{calc}) divided by the terminal rate constant (λ_z). C_{calc} and λ_z were both obtained by log-linear regression of the three last points of the concentration versus time curve. $AUMC_{0-\infty}$ is the area under the first moment versus time curve from time zero until infinity, which is the sum of $AUMC_{0-t}$ and the residual area $AUMC_{t-\infty}$. $AUMC_{t-\infty}$ was expressed as $C_{calc} \cdot t_{last}/\lambda_z + C_{calc}/\lambda_z^2$, where t_{last} is the time point of the last observation. k_0 is the rate of the infusion and T is the duration of the infusion. In Papers II and IV, the terminal half-life (t½) was derived from $\ln 2/\lambda_z$.

In Paper III, assessment of the partitioning between plasma and blood (C_{blood}/C_{plasma}) was calculated according to Eq. 10 (Tozer, 1981):

$$\frac{C_{blood}}{C_{plasma}} = 1 - H + H \cdot \frac{C_{RBC}}{C_{plasma}} \quad (10)$$

where C_{blood}, C_{plasma} and C_{RBC} are the oxycodone concentration in blood, plasma and red blood cells, respectively. H is the hematocrit, estimated to 42% in the rat (Leonard and Ruben, 1986).

In Paper III, comparisons on the influx clearance across the BBB based on unbound concentrations to the cerebral blood flow were made and the blood clearance across the BBB ($CL_{in,blood}$) was calculated using Eq. 11.

$$CL_{in,blood} = \frac{CL_{in} \cdot f_u}{\frac{C_{blood}}{C_{plasma}}} \quad (11)$$

CL_{in} and f_u are the final parameter estimates of the PK model in Paper III, and C_{blood}/C_{plasma} is calculated from Eq. 10.

The partitioning of drug between brain and blood at steady-state was calculated as

$$K_p \ ] \ \frac{C_{tot,brain}}{C_{plasma}} \quad (12)$$

$$K_{p,u} \ ] \ \frac{C_{tot,brain}}{C_u} \quad (13)$$

$$K_{p,uu} \ ] \ \frac{C_{u,brainISF}}{C_u} \quad (14)$$

where K_p is the partition coefficient between total brain concentrations ($C_{tot,brain}$) and total plasma concentrations (C_{plasma}). $K_{p,u}$ is the partition coefficient between total brain concentrations ($C_{tot,brain}$) and unbound blood concentrations (C_u) and $K_{p,uu}$ is the partition coefficient between unbound drug in interstitial fluid (ISF) and unbound drug in blood.

In Paper II, the total antinociceptive response of oxycodone was expressed as the area under the tail-flick latency versus time curve (AUEC).

Statistics

In Paper II, the PK parameters are presented as geometric means with confidence intervals (CIs). Plasma concentrations versus time curves are presented as geometric means and standard deviations (SDs). The CIs and SDs were derived from log-transformed data. The PK parameters of the study groups were compared using Wilcoxon's rank sum test (S-plus® 6.1 for Windows, Insightful Corp., Seattle, WA) based on non-transformed data.

In Paper II; total brain tissue concentrations and ratios of total brain tissue/plasma concentrations are presented as means and SDs. The groups were compared using an unpaired two-sided t-test (S-plus® 6.1 for Windows, Insightful Corp., Seattle, WA). In Paper III, K_p, $K_{p,u}$ and $K_{p,uu}$ are presented as mean with SDs.

The tail-flick latencies are presented as means and SDs (Paper II and IV). In Paper II, the tail-flick latencies of the two study groups were compared using a two-sided, unpaired t-test (S-plus® 6.1 for Windows, Insightful Corp., Seattle, WA). In Paper IV, the baseline latencies before and during the stabilization period were compared with a t-test (Microsoft® Office Excel 2003, Microsoft Corp.) with pair-wise comparisons to exclude any influence of the calibrators on the tail-flick latency.

In all statistical evaluations of the non-compartmental analysis, a p-value of less than 5 % was needed for statistical significance.

Modelling

The PK of oxycodone (Paper III) and morphine (Paper IV) and the PKPD of both drugs (Paper IV) were analyzed by nonlinear mixed effects modelling in NONMEM, version VIβ (GloboMax LLC, Hanover; MD, USA). Using this approach, the fixed effects that characterize the typical animal, and the random effects that characterize the inter-animal variability and residual variability could be estimated simultaneously. The first-order conditional estimation method with interaction

(FOCE INTER) was used throughout the modelling procedure. To distinguish between two nested models a drop in the OFV of 6.63 was required. This value (χ^2 distributed) corresponds approximately to $p < 0.01$ for one parameter difference. The need for inter-animal variability was investigated in all model parameters.

An exponential variance model was used to describe the inter-animal variability according to:

$$P_i = P_{pop} \cdot e^{\kappa_i} \quad (15)$$

where P_i and P_{pop} are the parameter in the i^{th} animal and the typical animal, respectively. η_i is the inter-animal variability, assumed to be normally distributed around zero and with a variance ω^2 to distinguish the i^{th} animal's parameter from the population mean. Additive, proportional and slope-intercept error models were considered for the residual variability.

The PK models of oxycodone (Paper III) and morphine (Paper IV) were based on the integrated blood-brain PK model for morphine with some modifications (Tunblad et al., 2004). For each drug, the blood probe recovery and blood dialysate data were combined and a sub-model was developed. Thereafter the total plasma concentration data was included and after that also the brain probe recovery data and the brain dialysate concentrations. One- and multi compartmental PK models were considered for both systemic and brain PK. Models allowing for a distribution delay between the arterial and venous parts of the central compartment were considered.

The BBB transport was parameterized in terms of CL_{in} and $K_{p,uu}$. For morphine, the earlier reported value of $V_{u,brain}$ of 1.7 ml/g brain was employed (Tunblad et al., 2003). For oxycodone, $V_{u,brain}$ was calculated from the animals decapitated at steady-state in the bolus + constant rate regimen (n = 5) in Paper III according to Eq. 5 and 10. The volume of blood in the rat brain was fixed to 14 µL/g brain (Bickel et al., 1996). The values of $V_{u,brain}$ for oxycodone and morphine were fixed in each PK model.

In Paper IV, the tail-flick latency was correlated to the unbound brain concentrations. Initially, separate PKPD models of oxycodone and morphine were developed and thereafter a joint PKPD model of both drugs was employed. By this manner, the model could be used as a statistical tool to evaluate if there were any differences in the PD parameters between the drugs. Direct effect, indirect effect and link models were evaluated. Linear, power and E_{max} models were considered to describe the data, and a power model according to Eq. 16 best described the data for both drugs.

$$Effect = Baseline + Slope \cdot C^{\gamma} \quad (16)$$

Effect is the tail-flick latency in seconds, Baseline is the tail-flick latency in the absence of drug and Slope is the slope of the concentration-effect relationship. C is the unbound concentration in brain of the drug and γ is a shape factor for the concentration-effect relationship.

Results and discussion

Chemical assay of oxycodone and metabolites (Paper I)

The analytical methods for analysis of oxycodone, oxymorphone and noroxycodone in Ringer, rat plasma and rat brain tissue were sensitive and reproducible. The linear dynamic range for Method I (Ringer) was 0.5-150 ng/mL, for Methods II and III (rat plasma) 0.5-250 ng/mL and for Method IV (rat brain tissue) 4-1000 ng/g brain tissue. Typical chromatograms are presented in Fig. 6.

The LLOQ of oxycodone, noroxycodone and oxymorphone in the described Methods I - III was 0.5 ng/mL. For all compounds and matrices, the CV and accuracy for this concentration was below 12 % and ±10 %, respectively. The LLOQ for Method IV was 20 ng/g tissue for oxycodone with a CV of 4 % and an accuracy of less than ±1 %. The LLOQ for noroxycodone and oxymorphone was 4 ng/g brain tissue, with a CV of less than 6 % and an accuracy of ±3 %.

For all analytes, concentrations and matrices described, the intra-day precision and accuracy were <11.3 % and <±14.9 %, respectively and the inter-day precision was <14.9 % and inter-day accuracy was <±6.5 %.

Influence of PSC833 on the PK and PD of oxycodone (Paper II)

The plasma PK and PD measured as tail-flick latency after oxycodone administration in the presence or absence of the P-gp inhibitor PSC833 was analyzed with a non-compartmental approach. The plasma concentration-time profiles of the two groups are shown in Fig. 7. There were no statistically significant differences between the two groups in $AUC_{0-\infty}$, CL, V_{ss} or t½ (Table 4), showing that oxycodone systemic pharmacokinetics is unaffected by P-gp inhibition.

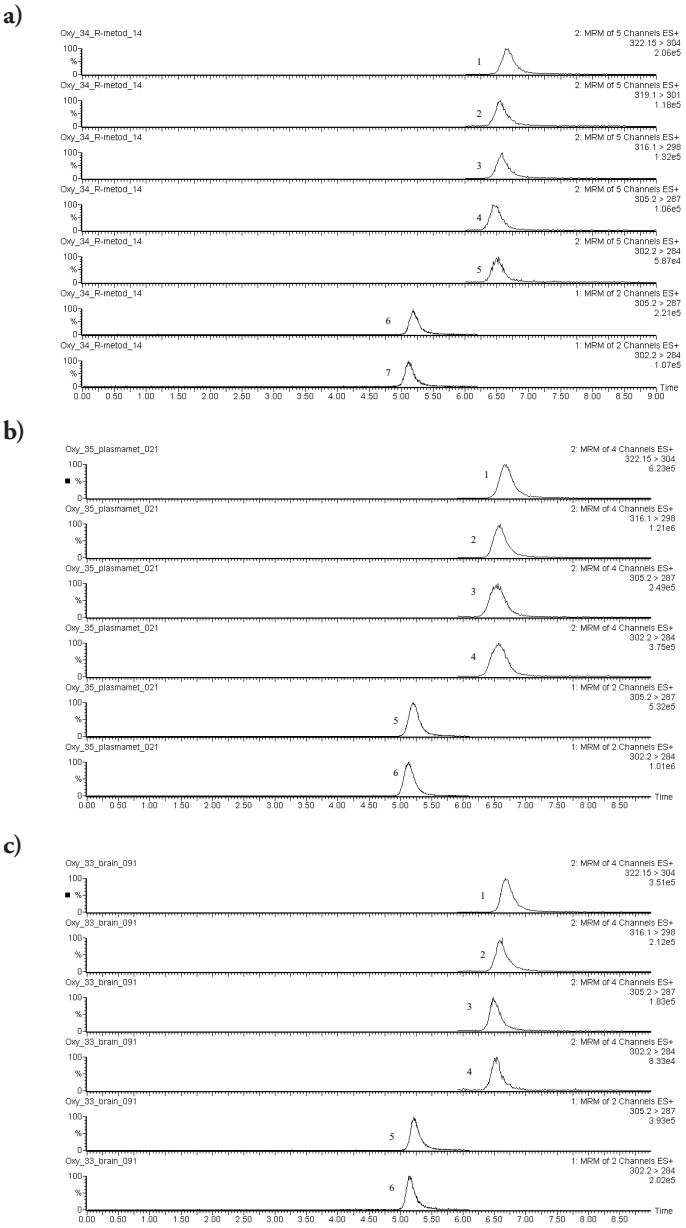

Figure 6. Typical chromatograms of (a) Ringer spiked with 20 ng/mL oxycodone (3), noroxycodone (5), oxymorphone (7), D3-oxycodone (2) and the internal standards D6-oxycodone (1), D3-noroxycodone(4) and D3-oxymorphone (6), (b) rat plasma using Method III spiked with 100 ng/mL oxycodone (2), noroxycodone (4), oxymorphone (6) and the internal standards D6-oxycodone (1), D3-noroxycodone (3) and D3-oxymorphone(5), (c) rat brain tissue spiked with 100 ng/g brain tissue of oxycodone (2), noroxycodone (4), oxymorphone (6) and the internal standards D6-oxycodone (1), D3-noroxycodone (3) and D3-oxymorphone (5).

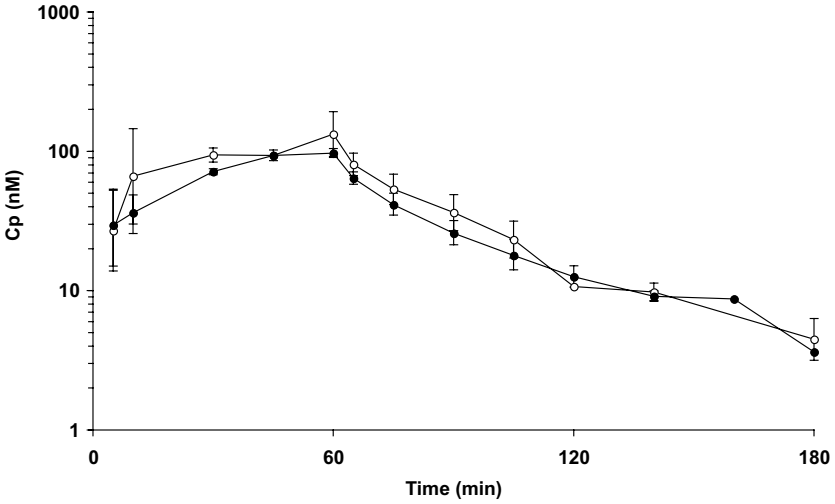

Figure 7. The total plasma concentration versus time profile following a 0.3 mg/kg 60 minute constant rate infusion of oxycodone to rats with (○)and without (●) coadministration of PSC833. Data are presented as geometric means and SDs.

Table 4. *The pharmacokinetic parameters of oxycodone in rats based on plasma observations. The data is presented as geometrical means and 95 % confidence intervals. The p-value was calculated using Wilcoxon's rank test.*

	Oxycodone + PSC833	**Oxycodone + vehicle**	**p-value**
AUC (h ⊥ng/ mL)	44.3 (34.8-56.6)	37.3 (33.8-41.3)	0.195
CL (L / hr)	1.85 (1.52-2.25)	2.26 (2.12-2.40)	0.195
V_{ss} (L)	0.97 (0.69-1.37)	1.16 (1.02-1.32)	0.721
t½ (hr)	0.37 (0.30-0.44)	0.36 (0.32-0.40)	0.574

The total brain tissue concentrations at 180 minutes after start of the infusion did not differ between the PSC833 treated and control groups, nor did the total concentration ratio between brain tissue and plasma. The lack of difference between the groups in brain tissue concentrations and in the ratio of the brain tissue/ plasma concentrations indicates that oxycodone BBB transport and brain tissue binding is not affected by P-gp inhibition.

There was no statistically significant difference in the peak tail-flick latency or AUEC between the two study groups (Fig. 8). This was in accordance with the unaltered brain concentrations of oxycodone in the presence of PSC833, and further indicated that oxycodone BBB transport is not affected by P-gp.

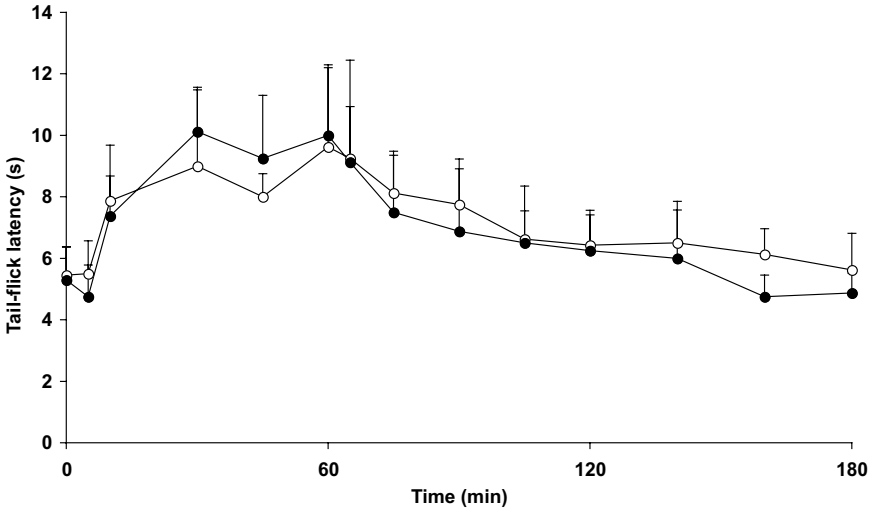

Figure 8. The tail-flick latency versus time profile after a 0.3 mg/kg 60 minute constant rate intravenous infusion of oxycodone with (○) and without (●) co-treatment with PSC833. Data are presented as means and SDs.

One of the challenges when studying the BBB transport of drugs *in vivo* using transporter inhibitors is the lack of specificity of the blocker to act at only one transporter. PSC833 is a cyclosporine analogue that have been extensively used to study the influence of P-gp in the BBB transport of diverse types of drugs such as M6G, digoxin and paclitaxel (Mayer et al., 1997; Fellner et al., 2002; Lotsch et al., 2002). However, PSC833 have also shown to be a moderate inhibitor of MRP2 and BCRP (Chen et al., 1999; Eisenblätter et al., 2003).

The tail-flick latency of the rat that received methadone and vehicle decreased rapidly after the stop of the infusion, while the rat that received methadone and PSC833 co-treatment had the maximally allowable 15 s tail flick latency for 60 min after the end of the infusion. Also, the same dose of PSC833 that was administered in Paper II resulted in a three-fold increase of brain concentrations of colchicine in rats (Desrayaud et al., 1997). Combined, it is clear that the dose of PSC833 administered in Paper II should be high enough to inhibit the BBB transport of oxycodone. The results of Paper II indicate that oxycodone is not a P-gp substrate in rats. This may have clinical implications as oxycodone may not interact with co-administered P-gp substrates at the BBB as opioids known to be P-gp substrates, i.e. methadone and fentanyl (Thompson et al., 2000; Wang et al., 2004).

Oxycodone and morphine PK (Paper III and IV)

The PK of oxycodone and morphine, including the BBB transport parameters CL_{in} and $K_{p,uu}$, was estimated using population nonlinear mixed effects modelling in NONMEM.

A two-compartment model which allowed for a delay between the venous and arterial compartments best described the PK for oxycodone in blood and plasma, while a one-compartment model was sufficient to describe the PK in the brain (Fig. 9 a). For morphine, a two-compartment model with a joint central compartment was applied to describe the PK of morphine in blood and plasma and a two-compartment model was needed to accurately describe the brain PK (Fig. 9 b). A summary of the PK parameters of oxycodone and morphine is shown in Table 5. The oxycodone data supported inter animal variability in blood and brain recovery, CL, V_c and f_u, while the morphine data supported inter animal variability in blood and brain recovery, V_c, inter-compartmental clearance (Q) and f_u.

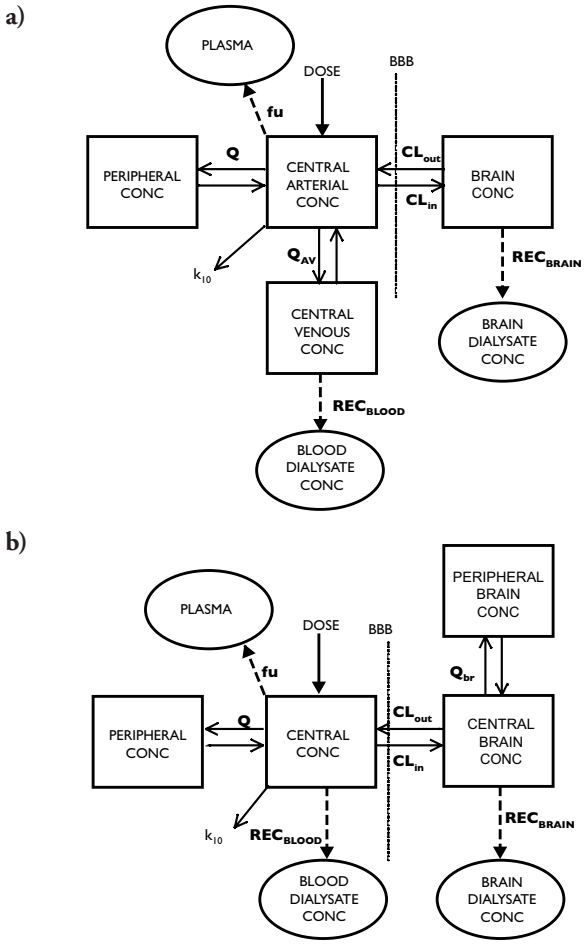

Figure 9. A schematic view of the final oxycodone (a) and morphine (b) PK models presented in Paper III and IV. The circles represent the observed data and the dashed arrows show the corrections that were made within the model to obtain the unbound drug concentrations in brain and blood. Thin arrows represent mass transport. The central compartment was a single compartment in the morphine model, but divided into an arterial and a venous part in the oxycodone model. For morphine, two compartments were needed to describe the unbound concentrations in the brain, while for oxycodone, a single brain compartment was sufficient to describe the data. conc = unbound concentration.

For oxycodone, a slope intercept model was used to describe the brain dialysate data. Proportional error models were used to describe the residual variability in the blood dialysate and plasma data, respectively and additive error models were used to describe the residual variability in the blood and brain recovery data, respectively. For morphine, a joint slope-intercept model for all observation types was used to describe the residual error.

Table 5. *The parameter estimates of the final pharmacokinetic models of oxycodone and morphine with their respective relative standard error (RSE %). IIV = inter-animal variability. NA = not applicable.*

		OXYCODONE		**MORPHINE**	
		Estimate (RSE %)	**IIV (RSE %)**	**Estimate (RSE %)**	**IIV (RSE %)**
CL	(mL/min)	37.4 (3.4)	0.14 (33)	34.7 (3.7)	
V_c	(mL)	1010 (5)	0.16 (36)	1130 (9.7)	0.71 (31)
Q	(mL/min)	4.37 (19)		2.96 (21)	0.44 (82)
V_{per}	(mL)	230 (13)		583 (7.2)	
Q_{AV}	(mL/min)	45.1 (7.9)		NA	
f_u	(%)	74.3 (7.1)	0.28 (51)	40.5 (15)	0.21 (42)
REC_{blood}	(%)	65.8 (2.3)	0.1 (28)	57.7 (8.9)	0.62 (22)
REC_{brain}	(%)	16.4 (6)	0.22 (31)	7.6	0.54 (46)
CL_{in}	(µL/min g brain)	1910 (20)		19.3 (17)	
$K_{p,uu}$		3.03 (3.8)		0.56 (20)	
Q_{br}	(µL/min g brain)	NA		37.1 (15)	
RESIDUAL VARIABILITY					
$\phi_{prop,plasma}$	(%)	19.5 (9.3)			
$\phi_{prop,blood}$	(%)	17.1 (8.1)			
$\phi_{prop,brain}$	(%)	15.2 (18)			
$\phi_{add,\ brain}$	(mg/mL)	0.226 (42)			
$\phi_{add,RECblood}$	(mg/mL)	2.44 (12)			
$\phi_{add,RECbrain}$	(mg/mL)	2.07 (12)			
ϕ_{prop}	(%)			20.7 (9.9)	
ϕ_{add}	(πM)			0.001 (30)	

BBB transport of oxycodone and morphine

The observed unbound oxycodone concentrations in brain and blood for the bolus + constant rate regimen are presented in Fig. 10 a. Equilibrium was rapidly reached between brain and blood. Surprisingly, the unbound brain concentrations were higher than the unbound blood concentration, indicating active influx at the BBB.

The higher unbound concentration in brain than in blood was also observed in the constant rate infusion regimen (Fig. 10 b). The unbound concentrations in brain and blood declined in parallel with half-lives of 40±8 min and 33±5 minutes, respectively. The oxycodone half-life in total brain tissue was 35 min, similar to the half-life in unbound brain ISF and blood (Fig. 10 b).

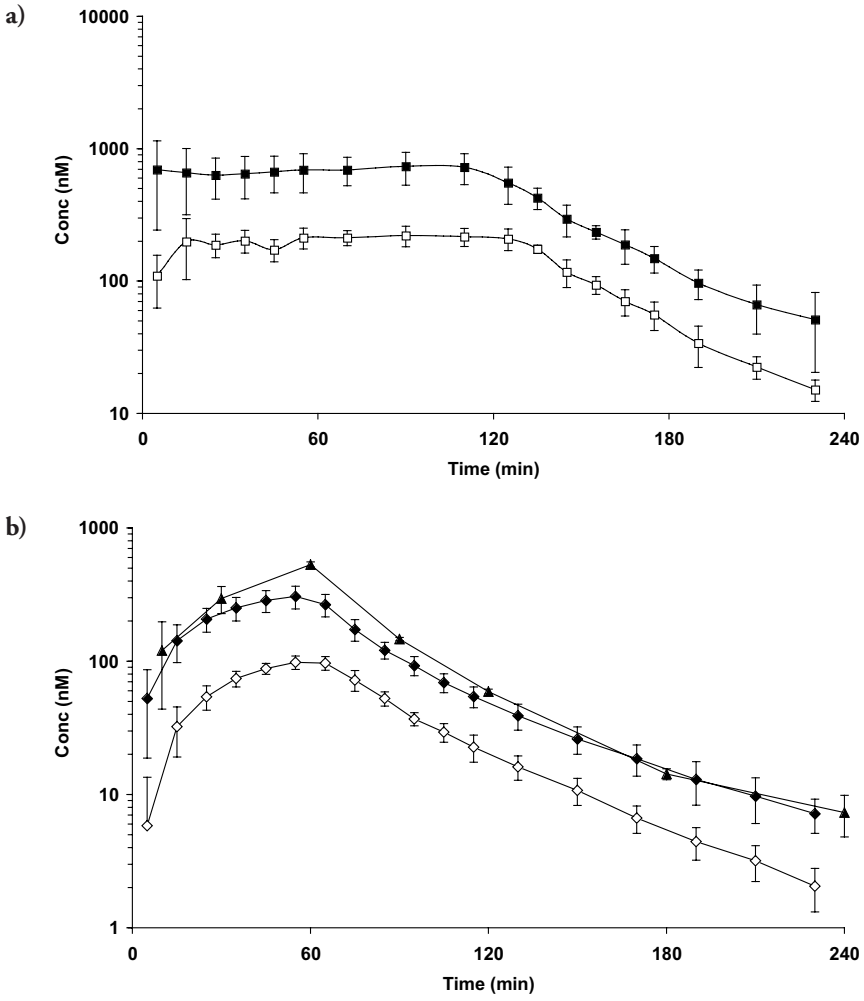

Figure 10. Observed concentration-time profiles of unbound oxycodone in brain (■) and blood (□) of rats in the bolus + constant rate regimen (n = 10) (a), and the unbound concentrations in brain (◆) and blood (◇) (n = 10) and total brain tissue concentrations (▲) (n = 3 per time point) from the animals receiving the constant rate regimen (b). Data are presented as means and SDs.

The observed unbound morphine concentrations in brain and blood, and the total brain concentrations versus time after the 60 minute constant rate infusion are shown in Fig. 11. Here, the unbound concentration in brain was lower than the unbound concentrations in blood, indicating active efflux at the BBB. After peaking at 60 min, the morphine concentrations in total brain tissue declined with a half-life of 65 min, the half-life of unbound morphine in brain was 68±18 min, i.e. longer than the half-life in blood of 38±8 min.

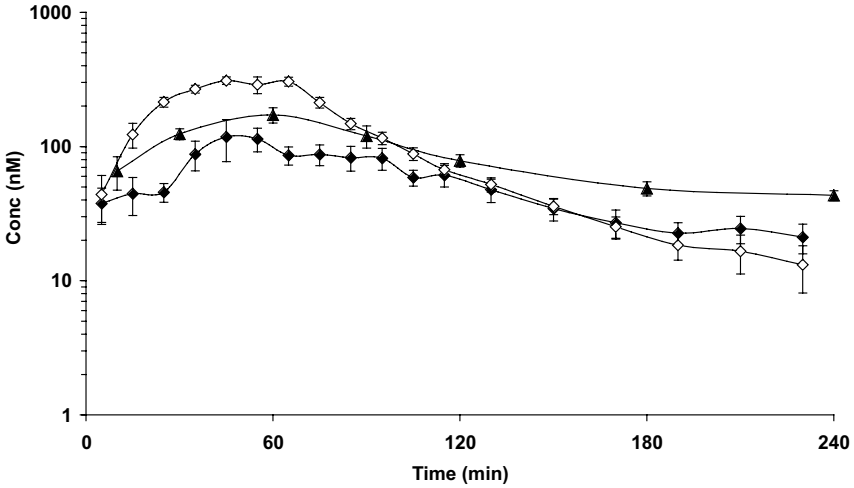

Figure 11. Observed unbound concentrations in brain (◆) and blood (◇) (n = 9) and total brain tissue concentrations (▲) (n = 3 per time point) in rats receiving 0.9 mg/kg morphine given as a 60 minute constant rate infusion. Data are presented as means and SDs.

Rate of BBB transport

The rate of transport across the BBB, expressed as the influx clearance (CL_{in}) was estimated to 1910 µL/min·g brain for oxycodone (Table 5), resulting in a rapid rate of equilibration across the BBB. The CL_{in} of oxycodone was much greater than the estimated value for morphine from Paper IV, and the reported values for M6G and M3G of 19.3, 1.66 and 0.11 µL/min·g brain, respectively (Xie et al., 2000; Tunblad et al., 2005). The reported CL_{in} of fentanyl from in situ brain perfusion studies of 1840 µL/min·g brain is in the same range as that of oxycodone. The cerebral blood flow has been reported to be 1440 µL/min·g brain (Shockley and LaManna, 1988). Recalculating oxycodone CL_{in} to the blood clearance across the BBB, $CL_{in,blood}$ resulted in a value of 1092 µL/min·g brain, making oxycodone a drug of medium extraction into the brain (correction from Paper III).

Extent of BBB transport

The extent of oxycodone BBB transport, expressed as $K_{p,uu}$ was estimated to 3.03 for oxycodone and 0.56 for morphine (Table 5).

A $K_{p,uu}$ greater than one shows that influx mechanisms contribute to the net flux of oxycodone across the BBB to a greater extent than possible efflux mechanisms. Some drugs are transported into the brain by influx mechanisms, including M6G and L-dopa (Kageyama et al., 2000; Bourasset et al., 2003). There are reports that some peptides (Thomas et al., 1997), fentanyl (Henthorn et al., 1999), gabapentin (Luer et al., 1999) and pentazocine (Suzuki et al., 2002) use saturable mechanisms to enter the brain. However, a $K_{p,uu}$ above unity has only been reported in very few investigations, including Paper III. The $K_{p,uu}$ for the R- and S-enantiomers of apomorphine was reported to be 12 and 5, respectively (Sam et al., 1997). This indicates that the net flux of apomorphine is also dominated by influx mechanisms. The intriguing results of a $K_{p,uu}$ greater than one may give incitements to drug development of a possible mechanism that may be used to increase drug distribution to the brain.

Morphine had a $K_{p,uu}$ of less than one, which make efflux transporters contribute to the net flux to a greater extent than possible influx mechanisms. Indeed, morphine has shown to be a substrate for P-gp and probenecid sensitive efflux transporters at the BBB (Letrent et al., 1999; Zong and Pollack, 2000; Tunblad et al., 2003).

Binding within the brain

The oxycodone binding within the brain, expressed as $V_{u,brain}$, was in Paper III calculated to 2.20 mL/g brain tissue. This was larger than the reported value of the brain interstitial space of 0.15 mL/g brain tissue (Goodman et al., 1973), which shows that oxycodone is distributed intracellularly and/or binds to tissue components.

PKPD of oxycodone and morphine (Paper IV)

Using PKPD modelling the unbound brain concentrations were correlated to the tail-flick pharmacological response *in vivo* in order to evaluate if there were any differences in the PD parameters between the drugs. The final PK parameters from the respective PK model of each drug were fixed and used as an input function in the PKPD modelling. Firstly, each drug was modelled separately and finally a joint PKPD model for oxycodone and morphine was developed.

In the separate modelling as well as in the joint PKPD model, neither of the drugs showed a delay between the unbound brain concentration and effect, making a direct effect model adequate to describe the concentration-effect relationship.

For both oxycodone and morphine, a power model according to Eq. 16 resulted in the best fit. The Slope and γ parameters were significantly different between the two drugs, but there was no difference in the Baseline parameter. The model supported joint inter-animal variability on Baseline and Slope. Inter-animal variability on γ was supported for oxycodone but not for morphine. The residual error was best described by a joint proportional error model for both drugs. The results from the best fit of the joint PKPD model are shown in Table 6.

The relationships for observed effect versus model predicted unbound brain and blood concentrations of oxycodone and morphine showed an interesting finding. A higher unbound oxycodone than morphine concentration in brain ISF was needed to exert an effect, while in blood, a higher unbound concentration of morphine was needed compared to oxycodone (Fig. 12 a and b). That is, if unbound brain ISF data had not been available, the concentration acting at the receptor would not be known, and the conclusion that oxycodone was more potent than morphine would have been drawn.

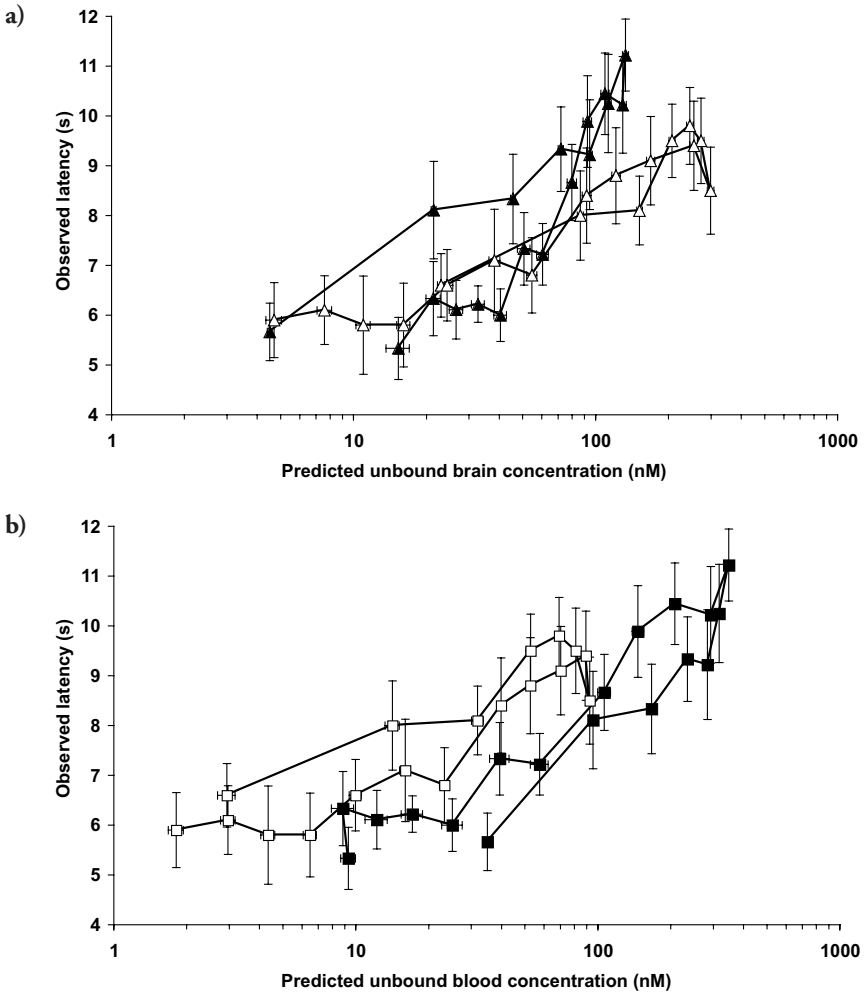

Figure 12. PKPD relationships of unbound oxycodone (open) and morphine (closed) in brain (a) and blood (b). The average observed latencies with standard errors of the means (SEMs) are plotted against the average PK model predicted unbound concentrations in brain and blood with SEMs.

Due to that two parameters (Slope and γ) were different between the drugs, the relative potency of the drugs was concentration-dependent. At an unbound brain ISF concentration of 55 nM the same tail-flick latency of 7.7 s was achieved, that is, the drugs were equipotent. Morphine was more potent than oxycodone at concentrations above 55 nM, while at concentrations below 55 nM, oxycodone was more potent than morphine (Fig. 13).

Table 6. *The parameter estimates of the final joint PKPD model of oxycodone and morphine with relative standard errors (RSE %). A power function according to Effect = Baseline + Slope · C$^{\gamma}$ best described the data, where Effect is the tail-flick latency in seconds, Baseline is the tail-flick latency in absence of drug, C is the unbound brain ISF concentration, Slope is the slope factor of the PKPD relationship and γ is a shape factor, determining the shape of the curve. Oxy = oxycodone, Mor = morphine.*

Parameter		**Drug**	**Estimate (RSE %)**
Baseline	(s)	Oxy + Mor	4.95 (5.3)
Slope	(s/μM)	Oxy	8 (12)
Slope	(s/μM)	Mor	27.9 (18)
ι		Oxy	0.371 (21)
ι		Mor	0.801 (9.4)
Inter-animal variability			
ϑ Baseline		Oxy + Mor	0.243 (22)
ϑ Slope		Oxy + Mor	0.200 (63)
ϑ ι		Oxy	0.528 (96)
Residual variability			
ϕ_{prop}	(%)	Oxy + Mor	18.5 (4.6)

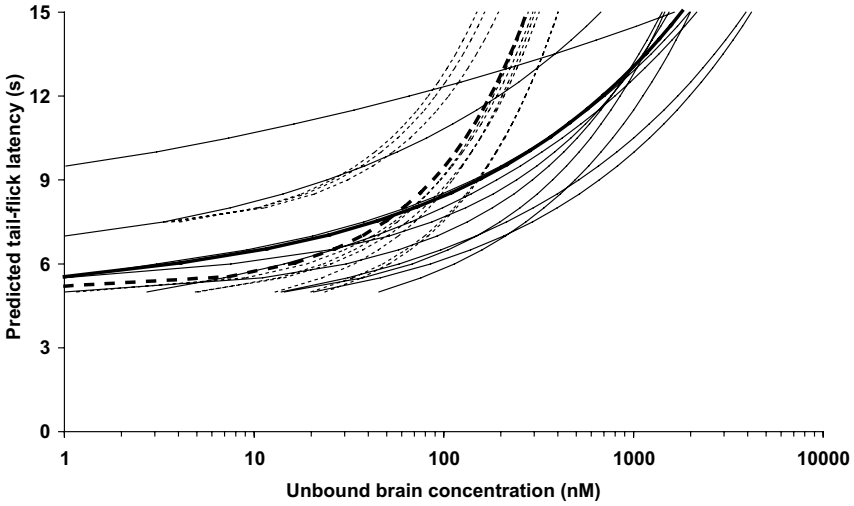

Figure 13. The simulated unbound concentration in brain ISF from tail-flick latencies ranging between baseline and cut-off (5 - 15 s) based on the individual parameter estimates from the PKPD model of oxycodone (solid line) and morphine (thin dashed line) and the typical individual for oxycodone (heavy solid line) and morphine (heavy dashed line).

In rat thalamus and cells transfected with μ-opioid receptors, 3-8 fold greater concentrations of oxycodone was needed for the same agonist mediated stimulation of [^{35}S]GTPγS binding as compared to morphine (Thompson et al., 2004; Lalovic et al., 2006; Peckham and Traynor, 2006). From these *in vitro* results, it would be expected that a 3-8 fold higher concentrations of oxycodone at the receptor would be needed to elicit the same G-protein activation as for morphine.

With this background it may be surprising that a higher dose of morphine was needed to elicit the same tail-flick latency as oxycodone in Paper IV. This is partly due to the higher unbound fraction of oxycodone as compared to morphine (74.3 % compared to 40.5 %, Paper III and IV), making a smaller fraction of morphine available for BBB transport. Also, based on the differences in $K_{p,uu}$ (3 and 0.56, respectively), the difference in the extent of BBB transport of unbound drug was approximately 6. Therefore, at a certain unbound blood concentration, a 6-fold higher brain ISF concentration of oxycodone will be observed compared to morphine. The unbound brain ISF concentration should be more closely related to the effect than the blood concentration as the μ-opioid receptors are located at the cell surface facing the ISF (Goodman and Gilman, 2001). By correlating the effects to the unbound concentrations in the brain ISF rather than the blood concentrations, a PKPD relationship that better describes the interaction with the receptor is obtained.

Conclusions

Characterization of the PK of a drug demands sensitive and selective analytical methods for determination of drug content in the collected samples. Methods for quantification of oxycodone, noroxycodone and oxymorphone and their deuterated analogues using LC/MS/MS in Ringer solution, rat plasma and rat brain tissue samples were developed and validated.

P-gp is known to restrict the entry of various drugs into the BBB, including opioids. Co-administration of the P-gp inhibitor PSC833 did not influence the systemic PK of oxycodone, nor did it influence the total brain tissue concentrations or the ratios of total brain tissue to plasma concentrations of oxycodone in rats. These results, in combination with the unaltered tail-flick latency when co-treated with PSC833, indicate that oxycodone is not a P-gp substrate in the rat. This may have clinical implications, as oxycodone is less likely to interact at the BBB with concomitantly administered P-gp substrates as other opioids.

Using microdialysis, the rate and extent of oxycodone transport across the BBB was assessed. The CL_{in} across the BBB was found to be very rapid. The $K_{p,uu}$ of oxycodone was found to be 3, meaning that the unbound brain ISF concentrations was 3-fold higher than the unbound blood concentrations. A $K_{p,uu}$ above one indicates that active influx processes are involved in the BBB transport of oxycodone. Knowledge on this transport process would give new incitements to drug development on how to increase delivery of drugs to the brain.

The PKPD of oxycodone and morphine was investigated. A direct effect model and a power function best described the data. The potency difference between the drugs was concentration dependent, with an infliction point of 55 nM, above which morphine was more potent, and below oxycodone was more potent. Oxycodone had a 6-fold higher $K_{p,uu}$ compared to morphine, which resulted in higher unbound brain ISF concentrations of oxycodone as compared to morphine based on the same unbound concentrations in blood.

Acknowledgements

This work was performed at the Department of Pharmaceutical Biosciences, Division of Pharmacokinetics and Drug Therapy, Uppsala University, Uppsala, Sweden.

I wish to express my sincere gratitude to everyone who has contributed to this thesis, and then especially:

My supervisors, Professor *Margareta Hammarlund-Udenaes* for sharing your scientific knowledge, for support and encouragement, and for always being positive and enthusiastic about my work. I also want to thank you for your understanding concerning the "family puzzle", and your advice on how to combine parenthood and work. My co-supervisor, Associate Professor *Ulrika Simonsson*, for all your bright ideas on statistics and modelling, and for always having the time when I need it. I greatly appreciate your support and engagement in my work, and for your understanding and advice on all sorts of things. I am grateful that I have had the opportunity to work with you both!

My co-author, *Britt Jansson*, for your enthusiasm and interesting discussions about the analytical world as well as the real one. You are one of the most quality conscious researchers I have met!

Jessica, for your skilful technical assistance, for always putting up with "just one more thing" and all the early mornings. This thesis would probably not be finished at all without your expertise. Many, many thanks!

Dr. *Anubha*, for being a great friend and for all our discussions concerning research and also the important things. Dr. *Karin,* for introducing me to the field of BBB and microdialysis. *Jörgen* for your friendship, for sharing your ideas and knowledge and always having time for discussions. You bring laughs to the division and time with you is never boring. *Markus* and *Stina* for your sharp ideas and interesting discussions. I have really enjoyed the experiences we all had together during travels as well as sharing the everyday life of being a PhD-student!

My master students *Malin Jönsson* and *Helén Merkell* for all the good work.

Marina, Marianne, Birgit and *Kjell* for all practical help at the division. *Karin* for making teaching so much easier.

Magnus Jansson for all your help and patience when putting the thesis together and

making it look the way it looks.

My former room-mate *Anders* for your friendship and all the good times we had (and have!) together. You always have the right words whenever I need it. My present room-mate, *Angelica*, for being such a positive and easygoing person and for always taking the time to explain NONMEM enigmas in an understandable manner.

Mia and *Bettan*, for your endless patience explaining things to me. You always have ideas on how to solve problems, and have kept med going when things have been rough.

All present and former colleagues at the division, for Christmas parties, fun lunches, go'fika raster, doktorand dagar, exciting travels and good meetings and seminars. You all create the best place to work in the world!

The Swedish Academy of Pharmaceutical Sciences for giving me to opportunity to attend valuable courses and conferences.

Jag vill också tacka min familj och mina vänner och då särskilt:

Maria, Ann-Marie, Emma och *Ulrika* med familjer, för att ni gör jobbet så mycket roligare och vardagen så mycket festligare. Det är extremt lyxigt att ha er så nära varje dag!

Flogsta-flickorna, Lotta och Tove för allt bus under åren - ni gör livet mycket glammigare och roligare!

Hasse, Lena, Anders och Olof – för er stora omtanke, alla sånger och all musik, sköna dagar på Rådom och för att ni tar så väl hand om Arvid!

Oskar och *Frida*, mina småsyskon, för att vi tar så väl hand om varandra, för stöd och uppmuntran och för att vi har så mycket roligt ihop!

Christina och *Bengt*, mina föräldrar. Tack för att ni alltid har trott på mig och det jag gör, och alltid sagt att jag kan bli vad jag vill. Ni betyder oerhört mycket för mig!

Arvid, min trollunge, för att du är solstrålen i mitt liv.

Fredrik, mitt livs kärlek. Du är mitt stöd, du gör mig glad och lycklig varenda dag. Du är bäst!

Emma

References

Abbott NJ (2004) Evidence for bulk flow of brain interstitial fluid: significance for physiology and pathology. *Neurochem Int* **45:**545-552.

Backlund M, Lindgren L, Kajimoto Y and Rosenberg PH (1997) Comparison of epidural morphine and oxycodone for pain after abdominal surgery. *J Clin Anesth* **9:**30-35.

Bengtsson J, Jansson B and Hammarlund-Udenaes M (2005) On-line desalting and determination of morphine, morphine-3-glucuronide and morphine-6-glucuronide in microdialysis and plasma samples using column switching and liquid chromatography/ tandem mass spectrometry. *Rapid Commun Mass Spectrom* **19:**2116-2122.

Benveniste H, Drejer J, Schousboe A and Diemer NH (1987) Regional cerebral glucose phosphorylation and blood flow after insertion of a microdialysis fiber through the dorsal hippocampus in the rat. *J Neurochem* **49:**729-734.

Bickel U, Schumacher OP, Kang YS and Voigt K (1996) Poor permeability of morphine 3-glucuronide and morphine 6-glucuronide through the blood-brain barrier in the rat. *J Pharmacol Exp Ther* **278:**107-113.

Bourasset F, Cisternino S, Temsamani J and Scherrmann JM (2003) Evidence for an active transport of morphine-6-beta-d-glucuronide but not P-glycoprotein-mediated at the blood-brain barrier. *J Neurochem* **86:**1564-1567.

Bouw MR and Hammarlund-Udenaes M (1998) Methodological aspects of the use of a calibrator in in vivo microdialysis-further development of the retrodialysis method. *Pharm Res* **15:**1673-1679.

Chen ZS, Kawabe T, Ono M, Aoki S, Sumizawa T, Furukawa T, Uchiumi T, Wada M, Kuwano M and Akiyama SI (1999) Effect of multidrug resistance-reversing agents on transporting activity of human canalicular multispecific organic anion transporter. *Mol Pharmacol* **56:**1219-1228.

Cisternino S, Mercier C, Bourasset F, Roux F and Scherrmann JM (2004) Expression, up-regulation, and transport activity of the multidrug-resistance protein Abcg2 at the mouse blood-brain barrier. *Cancer Res* **64:**3296-3301.

Curtis GB, Johnson GH, Clark P, Taylor R, Brown J, O'Callaghan R, Shi M and Lacouture PG (1999) Relative potency of controlled-release oxycodone and controlled-release morphine in a postoperative pain model. *Eur J Clin Pharmacol* **55:**425-429.

Dagenais C, Zong J, Ducharme J and Pollack GM (2001) Effect of mdr1a P-glycoprotein gene disruption, gender, and substrate concentration on brain uptake of selected compounds. *Pharm Res* **18:**957-963.

Davson H and Segal MB (1996) *Physiology of the CSF and blood-brain barriers*. CRC Press, Inc., Boca Raton.

de Lange EC, Hesselink MB, Danhof M, de Boer AG and Breimer DD (1995) The use of intracerebral microdialysis to determine changes in blood- brain barrier transport characteristics. *Pharm Res* **12:**129-133.

Deguchi Y (2002) Application of in vivo brain microdialysis to the study of blood-brain barrier transport of drugs. *Drug Metab Pharmacokinet* **17:**395-407.

DeHaven-Hudkins DL and Dolle RE (2004) Peripherally restricted opioid agonists as novel analgesic agents. *Curr Pharm Des* **10:**743-757.

Desrayaud S, Guntz P, Scherrmann JM and Lemaire M (1997) Effect of the P-glycoprotein inhibitor, SDZ PSC 833, on the blood and brain pharmacokinetics of colchicine. *Life Sci* **61:**153-163.

Dumez H, Guetens G, De Boeck G, Highley MS, de Bruijn EA, van Oosterom AT and Maes RA (2005) In vitro partition of irinotecan (CPT-11) in human volunteer blood: the influence of concentration, gender and smoking. *Anticancer Drugs* **16:**893-895.

Eisenblätter T, Huwel S and Galla HJ (2003) Characterisation of the brain multidrug resistance protein (BMDP/ABCG2/BCRP) expressed at the blood-brain barrier. *Brain Res* **971:**221-231.

Elmquist WF and Sawchuk RJ (1997) Application of microdialysis in pharmacokinetic studies. *Pharm Res* **14:**267-288.

Fellner S, Bauer B, Miller DS, Schaffrik M, Fankhanel M, Spruss T, Bernhardt G, Graeff C, Farber L, Gschaidmeier H, Buschauer A and Fricker G (2002) Transport of paclitaxel (Taxol) across the blood-brain barrier in vitro and in vivo. *J Clin Invest* **110:**1309-1318.

Gardmark M, Karlsson MO, Jonsson F and Hammarlund-Udenaes M (1998) Morphine-3-glucuronide has a minor effect on morphine antinociception. Pharmacodynamic modeling. *J Pharm Sci* **87:**813-820.

Goodman and Gilman (2001) *Goodman & Gilman´s The pharmacological basis of therapeutics*. The McGraw-Hill Companies, Inc.

Goodman FR, Weiss GB and Alderdice MT (1973) On the measurement of extracellular space in slices prepared from different rat brain areas. *Neuropharmacology* **12:**867-873.

Groothuis DR, Ward S, Schlageter KE, Itskovich AC, Schwerin SC, Allen CV, Dills C and Levy RM (1998) Changes in blood-brain barrier permeability associated with insertion of brain cannulas and microdialysis probes. *Brain Res* **803:**218-230.

Hammarlund-Udenaes M (2000) The use of microdialysis in CNS drug delivery studies. Pharmacokinetic perspectives and results with analgesics and antiepileptics. *Adv Drug Deliv Rev* **45:**283-294.

Hammarlund-Udenaes M, Paalzow LK and de Lange EC (1997) Drug equilibration across the blood-brain barrier--pharmacokinetic considerations based on the microdialysis method. *Pharm Res* **14:**128-134.

Henthorn TK, Liu Y, Mahapatro M and Ng KY (1999) Active transport of fentanyl by the blood-brain barrier. *J Pharmacol Exp Ther* **289:**1084-1089.

Joel SP, Osborne RJ and Slevin ML (1988) An improved method for the simultaneous determination of morphine and its principal glucuronide metabolites. *J Chromatogr* **430:**394-399.

Kageyama T, Nakamura M, Matsuo A, Yamasaki Y, Takakura Y, Hashida M, Kanai Y, Naito M, Tsuruo T, Minato N and Shimohama S (2000) The 4F2hc/LAT1 complex transports L-DOPA across the blood-brain barrier. *Brain Res* **879:**115-121.

Kakee A, Terasaki T and Sugiyama Y (1996) Brain efflux index as a novel method of analyzing efflux transport at the blood-brain barrier. *J Pharmacol Exp Ther* **277:**1550-1559.

Lalovic B, Kharasch E, Hoffer C, Risler L, Liu-Chen LY and Shen DD (2006) Pharmacokinetics and pharmacodynamics of oral oxycodone in healthy human subjects: role of circulating active metabolites. *Clin Pharmacol Ther* **79:**461-479.

Leonard R and Ruben Z (1986) Hematology reference values for peripheral blood of laboratory rats. *Lab Anim Sci* **36:**277-281.

Leow KP, Smith MT, Williams B and Cramond T (1992) Single-dose and steady-state pharmacokinetics and pharmacodynamics of oxycodone in patients with cancer. *Clin Pharmacol Ther* **52:**487-495.

Leow KP, Wright AW, Cramond T and Smith MT (1993) Determination of the serum protein binding of oxycodone and morphine using ultrafiltration. *Ther Drug Monit* **15:**440-447.

Letrent SP, Pollack GM, Brouwer KR and Brouwer KL (1998) Effect of GF120918, a potent P-glycoprotein inhibitor, on morphine pharmacokinetics and pharmacodynamics in the rat. *Pharm Res* **15:**599-605.

Letrent SP, Pollack GM, Brouwer KR and Brouwer KL (1999) Effects of a potent and specific P-glycoprotein inhibitor on the blood-brain barrier distribution and antinociceptive effect of morphine in the rat. *Drug Metab Dispos* **27:**827-834.

Lonnroth P, Jansson PA and Smith U (1987) A microdialysis method allowing characterization of intercellular water space in humans. *Am J Physiol* **253:**E228-231.

Lotsch J, Schmidt R, Vetter G, Schmidt H, Niederberger E, Geisslinger G and Tegeder I (2002) Increased CNS uptake and enhanced antinociception of morphine-6-glucuronide in rats after inhibition of P-glycoprotein. *J Neurochem* **83:**241-248.

Luer MS, Hamani C, Dujovny M, Gidal B, Cwik M, Deyo K and Fischer JH (1999) Saturable transport of gabapentin at the blood-brain barrier. *Neurol Res* **21:**559-562.

MacPherson RD (2002) New directions in pain management. *Drugs Today (Barc)* **38:**135-145.

Mayer U, Wagenaar E, Dorobek B, Beijnen JH, Borst P and Schinkel AH (1997) Full blockade of intestinal P-glycoprotein and extensive inhibition of blood-brain barrier P-glycoprotein by oral treatment of mice with PSC833. *J Clin Invest* **100:**2430-2436.

Murthy BR, Pollack GM and Brouwer KL (2002) Contribution of morphine-6-glucuronide to antinociception following intravenous administration of morphine to healthy volunteers. *J Clin Pharmacol* **42:**569-576.

Oguri K, Hanioka N and Yoshimura H (1990) Species differences in metabolism of codeine: urinary excretion of codeine glucuronide, morphine-3-glucuronide and morphine-6-glucuronide in mice, rats, guinea pigs and rabbits. *Xenobiotica* **20:**683-688.

Ohno K, Pettigrew KD and Rapoport SI (1979) Local cerebral blood flow in the conscious rat as measured with 14C- antipyrine, 14C-iodoantipyrine and 3H-nicotine. *Stroke* **10:**62-67.

Oldendorf WH (1970) Measurement of brain uptake of radiolabeled substances using a tritiated water internal standard. *Brain Res* **24:**372-376.

Peckham EM and Traynor JR (2006) Comparison of the antinociceptive response to morphine and morphine-like compounds in male and female sprague-dawley rats. *J Pharmacol Exp Ther* **316:**1195-1201.

Pessin JE and Bell GI (1992) Mammalian facilitative glucose transporter family: structure and molecular regulation. *Annu Rev Physiol* **54:**911-930.

Polli JW, Baughman TM, Humphreys JE, Jordan KH, Mote AL, Salisbury JA, Tippin TK and Serabjit-Singh CJ (2003) P-glycoprotein influences the brain concentrations of cetirizine (Zyrtec), a second-generation non-sedating antihistamine. *J Pharm Sci* **92:**2082-2089.

Poyhia R and Kalso EA (1992) Antinociceptive effects and central nervous system depression caused by oxycodone and morphine in rats. *Pharmacol Toxicol* **70:**125-130.

Poyhia R, Seppala T, Olkkola KT and Kalso E (1992) The pharmacokinetics and metabolism of oxycodone after intramuscular and oral administration to healthy subjects. *Br J Clin Pharmacol* **33:**617-621.

Sam E, Sarre S, Michotte Y and Verbeke N (1997) Distribution of apomorphine enantiomers in plasma, brain tissue and striatal extracellular fluid. *Eur J Pharmacol* **329:**9-15.

Sawchuk RJ and Elmquist WF (2000) Microdialysis in the study of drug transporters in the CNS. *Adv Drug Deliv Rev* **45:**295-307.

Shockley RP and LaManna JC (1988) Determination of rat cerebral cortical blood volume changes by capillary mean transit time analysis during hypoxia, hypercapnia and hyperventilation. *Brain Res* **454:**170-178.

Silvasti M, Rosenberg P, Seppala T, Svartling N and Pitkanen M (1998) Comparison of analgesic efficacy of oxycodone and morphine in postoperative intravenous patient-controlled analgesia. *Acta Anaesthesiol Scand* **42:**576-580.

Skarke C, Jarrar M, Schmidt H, Kauert G, Langer M, Geisslinger G and Lotsch J (2003) Effects of ABCB1 (multidrug resistance transporter) gene mutations on disposition and central nervous effects of loperamide in healthy volunteers. *Pharmacogenetics* **13:**651-660.

Suzuki T, Oshimi M, Tomono K, Hanano M and Watanabe J (2002) Investigation of transport mechanism of pentazocine across the blood-brain barrier using the in situ rat brain perfusion technique. *J Pharm Sci* **91:**2346-2353.

Takasato Y. Rapoprt S *An in situ brain perfuion technique to study cerebrovascular transport in the rat*.

Tamai I and Tsuji A (2000) Transporter-mediated permeation of drugs across the blood-brain barrier. *J Pharm Sci* **89:**1371-1388.

Thomas SA, Abbruscato TJ, Hruby VJ and Davis TP (1997) The entry of [D-penicillamin e2,5]enkephalin into the central nervous system: saturation kinetics and specificity. *J Pharmacol Exp Ther* **280:**1235-1240.

Thompson CM, Wojno H, Greiner E, May EL, Rice KC and Selley DE (2004) Activation of G-proteins by morphine and codeine congeners: insights to the relevance of O- and N-demethylated metabolites at mu- and delta-opioid receptors. *J Pharmacol Exp Ther* **308:**547-554.

Thompson SJ, Koszdin K and Bernards CM (2000) Opiate-induced analgesia is increased and prolonged in mice lacking P-glycoprotein. *Anesthesiology* **92:**1392-1399.

Tozer TN (1981) Concepts basic to pharmacokinetics. *Pharmacol Ther* **12:**109-131.

Tunblad K, Hammarlund-Udenaes M and Jonsson EN (2004) An integrated model for the analysis of pharmacokinetic data from microdialysis experiments. *Pharm Res* **21:**1698-1707.

Tunblad K, Hammarlund-Udenaes M and Jonsson EN (2005) Influence of probenecid on the delivery of morphine-6-glucuronide to the brain. *Eur J Pharm Sci* **24:**49-57.

Tunblad K, Jonsson EN and Hammarlund-Udenaes M (2003) Morphine blood-brain barrier transport is influenced by probenecid co-administration. *Pharm Res* **20:**618-623.

Ungerstedt U (1991) Microdialysis--principles and applications for studies in animals and man. *J Intern Med* **230:**365-373.

van Bree JB, de Boer AG, Danhof M, Ginsel LA and Breimer DD (1988) Characterization of an "in vitro" blood-brain barrier: effects of molecular size and lipophilicity on cerebrovascular endothelial transport rates of drugs. *J Pharmacol Exp Ther* **247:**1233-1239.

Wang JS, Ruan Y, Taylor RM, Donovan JL, Markowitz JS and DeVane CL (2004) Brain penetration of methadone (R)- and (S)-enantiomers is greatly increased by P-glycoprotein deficiency in the blood-brain barrier of Abcb1a gene knockout mice. *Psychopharmacology (Berl)* **173:**132-138.

Wang Y, Wong SL and Sawchuk RJ (1993) Microdialysis calibration using retrodialysis and zero-net flux: application to a study of the distribution of zidovudine to rabbit cerebrospinal fluid and thalamus. *Pharm Res* **10:**1411-1419.

Westerling D, Persson C and Hoglund P (1995) Plasma concentrations of morphine, morphine-3-glucuronide, and morphine- 6-glucuronide after intravenous and oral administration to healthy volunteers: relationship to nonanalgesic actions. *Ther Drug Monit* **17:**287-301.

Xie R, Bouw MR and Hammarlund-Udenaes M (2000) Modelling of the blood-brain barrier transport of morphine-3- glucuronide studied using microdialysis in the rat: involvement of probenecid-sensitive transport. *Br J Pharmacol* **131:**1784-1792.

Yeh SY, Gorodetzky CW and Krebs HA (1977) Isolation and identification of morphine 3- and 6-glucuronides, morphine 3,6-diglucuronide, morphine 3-ethereal sulfate, normorphine, and normorphine 6-glucuronide as morphine metabolites in humans. *J Pharm Sci* **66:**1288-1293.

Zong J and Pollack GM (2000) Morphine antinociception is enhanced in mdr1a gene-deficient mice. *Pharm Res* **17:**749-753.

Acta Universitatis Upsaliensis

Digital Comprehensive Summaries of Uppsala Dissertations from the Faculty of Pharmacy 50

Editor: The Dean of the Faculty of Pharmacy

A doctoral dissertation from the Faculty of Pharmacy, Uppsala University, is usually a summary of a number of papers. A few copies of the complete dissertation are kept at major Swedish research libraries, while the summary alone is distributed internationally through the series Digital Comprehensive Summaries of Uppsala Dissertations from the Faculty of Pharmacy. (Prior to January, 2005, the series was published under the title "Comprehensive Summaries of Uppsala Dissertations from the Faculty of Pharmacy".)

Distribution: publications.uu.se
urn:nbn:se:uu:diva-7772

ACTA
UNIVERSITATIS
UPSALIENSIS
UPPSALA
2007